

## Review article

# A comprehensive evaluation of solar cell technologies, associated loss mechanisms, and efficiency enhancement strategies for photovoltaic cells



Atib Mohammad Oni, Abu S.M. Mohsin\*, Md. Mosaddequr Rahman,  
Mohammed Belal Hossain Bhuiyan

*Department of Electrical and Electronic Engineering, Optics and Photonics Research Group, BRAC University, 66 Mohakhali, Dhaka 1212, Bangladesh*

## ARTICLE INFO

**Keywords:**  
 Photovoltaic cells  
 Silicon solar cell  
 Semiconductor solar cell  
 Novel material based solar cell  
 Loss mechanism and performance optimization techniques

## ABSTRACT

In-depth assessments of cutting-edge solar cell technologies, emerging materials, loss mechanisms, and performance enhancement techniques are presented in this article. The study covers silicon (Si) and group III-V materials, lead halide perovskites, sustainable chalcogenides, organic photovoltaics, and dye-sensitized solar cells. In this regard, promising architectural advancements with graphene and metamaterials are highlighted. The study also encompasses various types of losses, including intrinsic and extrinsic losses in single-junction solar cells. Additionally, it evaluates efficiency improvement techniques such as light management and spectral utilization. While the efficiency of Si-based solar cells has plateaued around 25%, the efficiency of III-V compound semiconductor-based multi-junction solar cells is increasing. However, the high material cost of III-V compound semiconductors is a drawback. Furthermore, CIGS and CdTe solar cell technologies compete with crystalline solar cells, owing to recent advances in cell performance, however environmental concerns and CdTe solar cells' low open-circuit voltage remain challenges. On the other hand, Perovskite solar cells are extremely efficient in both single and multijunction arrangements. Device deterioration, hysteresis, and film quality are among issues that must be addressed when industrialising perovskite solar cells.

## 1. Introduction

Solar energy usage is expanding quickly due to the negative effects of conventional fossil fuel-based energy sources on the environment (**Fig. 1a**). Solar energy is a reliable and abundant resource, and solar cells are an efficient and useful way to capture it. The sun delivers  $1367 \text{ W/m}^2$  of solar energy into the atmosphere (Liu, 2009). Nearly  $1.8 \times 10^{11} \text{ MW}$  of solar energy is absorbed globally, sufficient to cover the world's power requirement (Shah et al., 2015). At the end of 2022, the solar photovoltaic market saw growth to a record delivery capacity of 295 GW and the total installed PV capacity was more than 1.198 TW (Anon (2023a)). **Fig. 1b** illustrates that the annual capacity of PV generation is steadily increasing day by day. In 2022, following years of stagnation due to the COVID-19 pandemic, a record-breaking 9.5 million off-grid solar products with a combined capacity of 94 megawatts were sold, primarily comprising lighting products and various appliances (Feldman et al., 2023a). Experts forecast that the world will require 75 terawatts or more installed PV by 2050 to meet decarbonization goals (Haegel et al., 2023).

Over time, various types of solar cells have been built, each with unique materials and mechanisms. Silicon is predominantly used in the production of monocrystalline and polycrystalline solar cells (Anon, 2023a). The photovoltaic sector is now led by silicon solar cells because of their well-established technology and relatively high efficiency. Currently, industrially made silicon solar modules have an efficiency between 16% and 22% (Anon (2023b)). In contrast, thin-film solar cell technology utilizes materials such as amorphous silicon (a-Si) (Carlson and Wronski, 1976), cadmium sulfide (CdS) (Böer, 2011), cadmium telluride (CdTe) (Chu and Chu, 1993), copper indium gallium selenide (CIGS) (Rezaei et al., 2020), and various others. Solar cells of this kind, characterized by reduced material usage, lower manufacturing costs, and flexibility, typically achieve conversion efficiencies ranging from 6% to 15% (Jaiswal et al., 2022). At present, the objective of solar cell research is to improve cell efficiency and explore novel designs to reduce material usage and manufacturing costs. Some examples of advanced solar cell technologies are quantum-dot solar cells (Kamat, 2013), dye-sensitized solar cells (Sharma et al., 2018), organic-solar cells (Servaites et al., 2011), perovskite-solar cells (Anon, 2023a), and more.

\* Corresponding author.

E-mail address: [asm.mohsin@bracu.ac.bd](mailto:asm.mohsin@bracu.ac.bd) (A.S.M. Mohsin).

At present, crystalline silicon modules are less expensive than modules composed of other materials. The large production scale of silicon feedstock, wafers, cells, and modules is responsible for this cost advantage. NREL provides a summary of the production cost for the PV module in 2020 (Righini and Enrichi, 2020). According to the summary, the production cost of monocrystalline PERC is less than \$0.20/W<sub>(DC)</sub>. On the other hand, the cost is more than \$0.45/W<sub>(DC)</sub> for high-efficiency cells for UAV and space applications. In mid-2023, polysilicon spot prices experienced a sharp 70% decline, reaching the \$8/kg level for the first time in 3 years (Righini and Enrichi, 2020). Besides, global module prices reached an all-time low of \$0.17/W due to factors including oversupply, competitive pressures, falling commodities and freight costs, and a weakened yuan compared to the dollar, despite sustained high demand for modules worldwide (Feldman et al., 2023a). Data for eight of the top suppliers of PV modules showed that shipments in 2023 were 61% higher than the shipments from these businesses in 2022 (Feldman et al., 2023a).

The performance of PV cell and module technologies has been enhanced, and production prices have decreased, because of decades of research and development efforts. Fig. 2 provides an overview of the technological trends in crystalline-silicon (c-Si) photovoltaic (PV) modules, highlighting the key characteristics and features of the dominant technologies in the market at the time of the research. The use of bigger ingot and wafer sizes, the switch from full-area aluminum back surface field (Al BSF) to passivated emitter rear contact (PERC) manufacturing, and enhanced metallization and connectivity processes are all significant developments. Efficiency losses from cells to modules have been reduced overall as a result of these developments (Righini and Enrichi, 2020).

Numerous studies on various aspects of solar cells have been previously published. For example, a review paper by Righini et al. provides a quick overview of the history, solar cells types, and their present state (Roy et al., 2020). The evolution, fabrication techniques, and current status of perovskite solar cell is reviewed by Roy et al (Asim et al., 2012). The function of material science in solar cells was reviewed by Asim et al (Haug and Ballif, 2015). They discussed various solar cell structures, advanced high-efficiency concepts, and production costs. Several areas, including light management and spectral utilization, offer avenues to enhance solar cell efficiency. Numerous research papers explore diverse strategies for efficiency improvement. For instance, Haug et al. published a review paper on light management in thin-film silicon solar cell (Schmid, 2017). Light management in chalcopyrite type solar cell by using nanostructures is reviewed by Schimid M (Berry et al., 2022). Another review on light management techniques for perovskite solar cell is done by Berry et al (Baiju and Yarema, 2022). Moreover, multijunction solar cell technology can be used to utilize the solar spectrum.

The current status and challenges of multijunction solar cell technology is reviewed by Baiju et al (Siah Chehreh Ghadikolaei, 2021). Furthermore, Multiple researchers have conducted reviews on diverse cooling technologies that enhance the performance of solar cells. For instance, a review paper by Ghadikolaei provides an overview of various cooling technologies and their impact on the performance of commercially available photovoltaic (PV) cells (Anon (2002)).

While numerous researchers extensively report on individual aspects of solar cells, this review focuses on the evolution of solar cell technology, novel materials and technologies, intrinsic and extrinsic loss mechanisms, and various efficiency improvement methods—topics rarely found in a single paper. In this study, a comprehensive review of the different types of solar cells, their current status, and prospects are discussed. This review paper could assist the new PV researchers in knowing about ongoing research and emerging technologies about different types of solar cells.

## 2. Theoretical background

Solar cells harness energy from sunlight, which comprises photons distributed across various wavelengths influenced by factors such as location, time, and month (Green, 2012a). The AM1.5 G spectrum, which adheres to the ASTM standard G173 (Fig. 3h), encompasses both direct and diffuse light components (Green, 2012b). For terrestrial applications, it employs a 1000 W/m<sup>2</sup> integrated power rating (Becquerel, 1839). This light energy's ultimate purpose in solar cells is to create useful electrical energy. Producing electricity directly from light is known as photovoltaic energy conversion. The photovoltaic effect was initially discovered in 1839 by Alexandre Edmond Becquerel (Fonash, 2010). The ability of a material to absorb light and generate an electric current is referred to as the photovoltaic effect, illustrated in Fig. 3(a-f). Semiconductor materials primarily serve as the absorber layer in a solar cell.

According to a book by Fonash S (Parmis and Oldham, 2013), solar energy conversion involves four essential processes: 1) light absorption, 2) generation of electron-hole pairs, 3) selective transport of charges, and 4) recombination of electrons and holes, ultimately restoring the absorber to its ground state. The absorber material is composed of two types of semiconductors: N-type and P-type, forming a PN junction. When light strikes a PN junction, it absorbs photons with energy matching the semiconductor material's energy gap, resulting in the creation of electrons and holes as charge carriers. In both inorganic and organic solar cells, it's crucial to separate these electrons and holes to prevent recombination, which would otherwise lead to energy loss without contributing to electricity generation. For inorganic solar cells, the PN junction establishes a built-in potential that facilitates

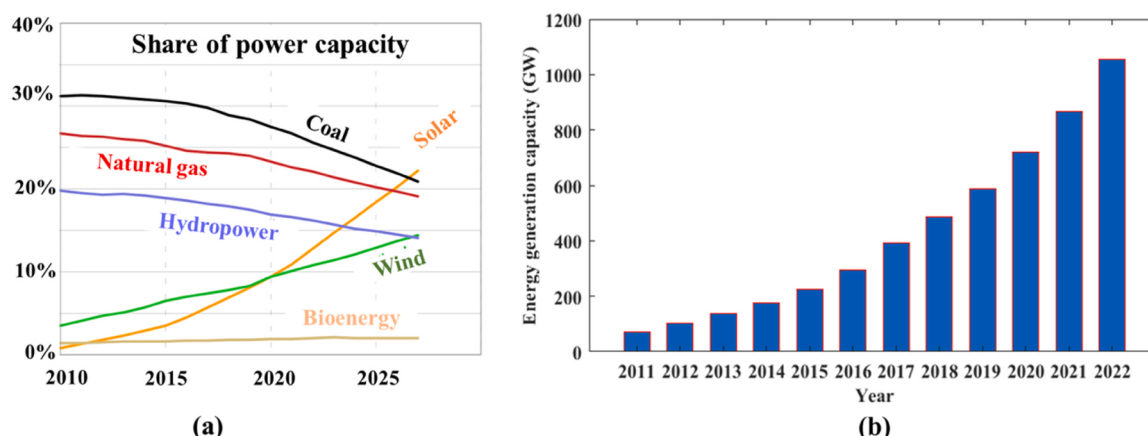


Fig. 1. a) Renewable energy sources are expanding their share of power capacity (Feldman et al#, 2023b). b) Capacity of photovoltaic energy generation with time (Woodhouse et al#, 2023).

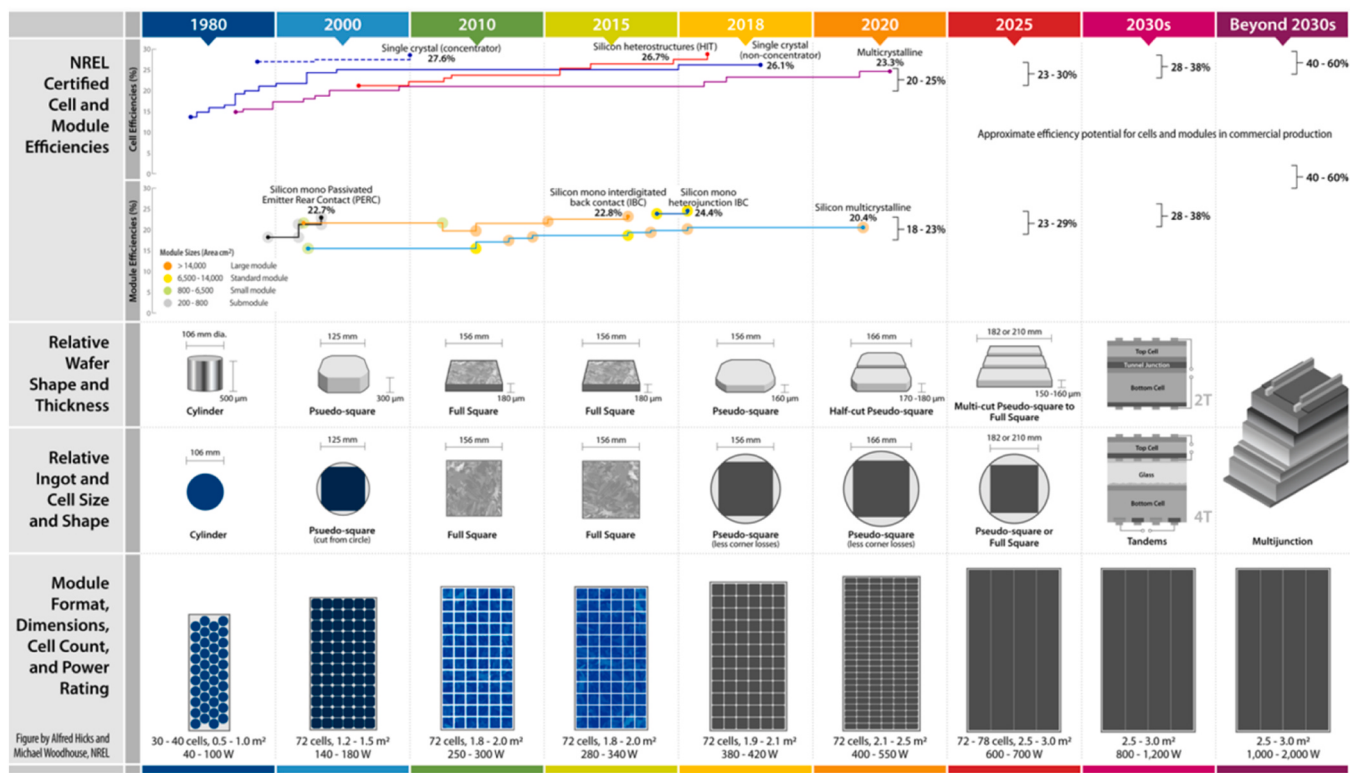


Fig. 2. PV cell and module technology progress (Righini and Enrichi, 2020).

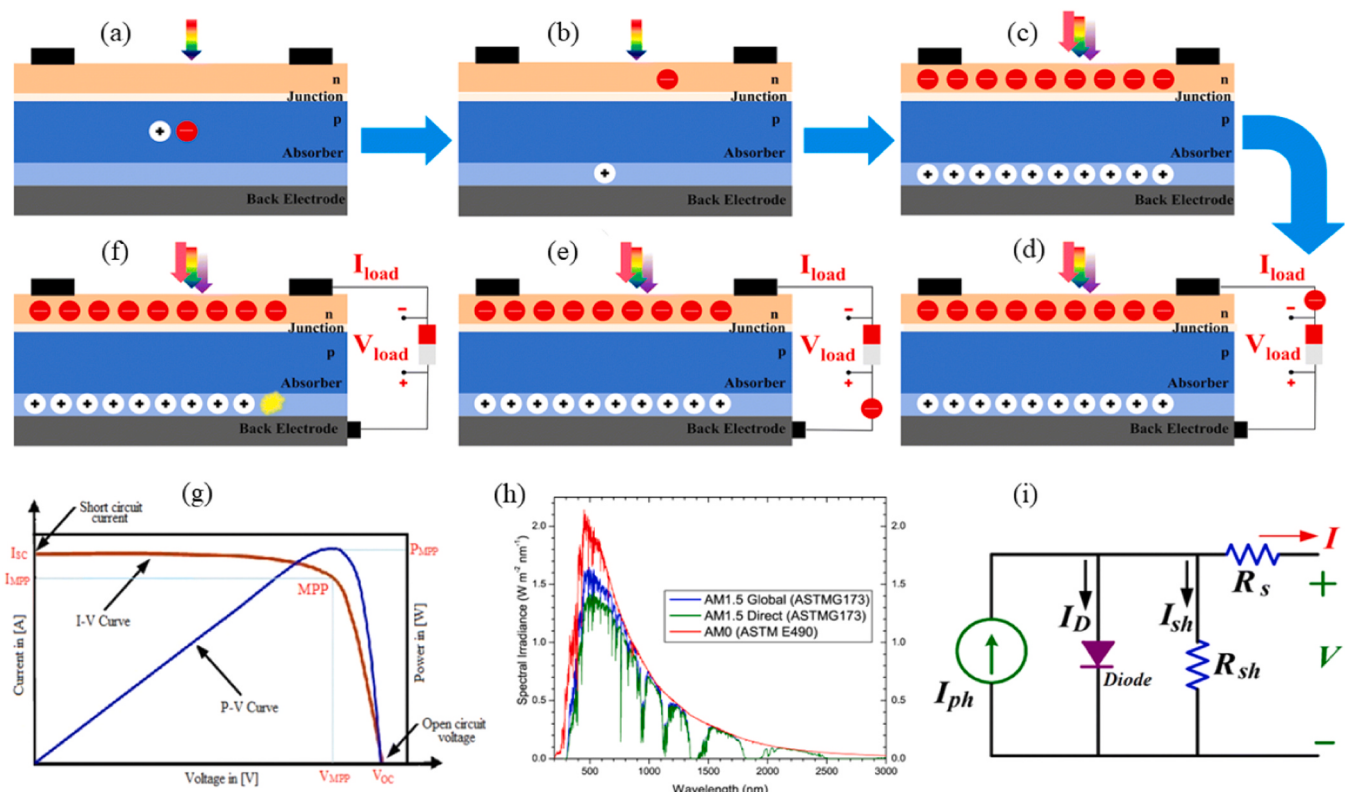


Fig. 3. Process of photovoltaic energy conversion (a-f) (Mohamed and Abd El Sattar, 2019). (a) Absorption, (b) separation of charge carriers, (c) continuous generation and separation, (d) connection of external load, (e) the transfer of a charge carrier from high to low potential, (f) recombination of carriers, g) J-V curve with key points, h) the ASTM standard G173-based AM1.5 G spectrum (Reused with permission from Ref (Green, 2012b). Copyright © 2012, John Wiley and Sons), i) equivalent electrical model of a solar cell (Kirchartz and Rau, 2018).

electron-hole separation. Conversely, in organic solar cells, excitons are conveyed to the appropriate electrodes through a specific process that facilitates electron or hole transfer (Parnis and Oldham, 2013). The electric field directs the separated electrons and holes to a certain location. The electrical energy produced as electrons flow is collected by metal connections at the photovoltaic cell's front and rear. The produced electricity can be captured and used for various purposes, including feeding it into the electrical grid or powering electrical devices.

The total power of incident light, the electrical output of the cell, efficiency, and fill factor are crucial parameters of a solar cell, and Table 1 contains the formulas. The incoming energy must be integrated across time, space, and bandwidth throughout the whole photon spectrum to determine the total power ( $P_{IN}$ ) incident on a solar cell. In Equation (1) the formula for  $P_{IN}$  is given. The electrical power ( $P_{OUT}$ ) can be obtained by multiplying the current ( $J$ ) and voltage ( $V$ ). In Equation (2), the current density  $J$  is defined as  $I$  divided by the cell area to express the output in per unit area. The  $I$ - $V$  curve of a cell and operating points are illustrated in Fig. 3g. The two extreme scenarios are represented by the points  $I_{SC}$  and  $V_{OC}$ :  $V_{OC}$  denotes open-circuit voltage, whereas  $I_{SC}$  indicates short-circuit current. Moreover, the efficiency of a solar cell is the ratio of electrical output at maximum power point (MPP) and total power of incident light. The electrical output at the maximum power point can be obtained by multiplying the current ( $J_{mp}$ ) and the voltage ( $V_{mp}$ ) of the cell at MPP. Therefore, the efficiency  $\eta$  can be expressed as Equation (3). However, this equation is only applicable if the total area where the light falls is being used to generate current. If the usable area for generating current is less than the total area where the light is striking, Equation (3) can be substituted with Equation (4). To evaluate how closely a solar cell mimics an ideal source, the fill factor (FF) has been coined. FF can be expressed as Equation (5).

In a solar cell, the absorption coefficient quantifies the material's effectiveness in absorbing incoming photons of light. It denotes how quickly light is absorbed as it travels through the substance. The absorption coefficient is commonly represented by the symbol  $\alpha(\lambda)$  and is defined as the reciprocal of the distance over which light intensity  $I_0(\lambda)$  falls by a factor of  $e$  (the base of natural logarithm). The intensity  $I(\lambda, x)$  at some point  $x$  can be determined by the Beer-Lambert law in the material (Aroutiounian et al., 2001). The Equation (6) can be used to measure the amount of light absorbed per unit distance traveled. The electron-hole production rate at a depth  $x$  can be calculated using Equation (7) for incoming light with wavelength  $\lambda$  and flux  $\phi_0$  Rehman et al., (2023).

**Table 1**  
Formulas for important parameters of solar cell.

Equation no.	Parameter	Formula	Nomenclature	Ref.
1	Total power of incident light	$P_{IN} = \int \frac{hc}{\lambda} \phi_0(\lambda) d\lambda$	$P_{IN}$ = Total power of incident light $\lambda$ = Wavelength of light $\phi_0(\lambda)$ = Photon Flux $h$ = Planck's constant $c$ = Speed of light	(Fritts and Fritts, 1883)
2	Electrical output power	$P_{OUT} = JV$	$P_{OUT}$ = Output power $J$ = Current density ( $A/m^2$ ) $V$ = Voltage across the cell (V)	(Parnis and Oldham, 2013)
3	Cell efficiency	$\eta = \frac{(J_{mp} V_{mp})}{P_{IN}}$	$\eta$ = Cell efficiency $J_{mp}$ = Maximum current $V_{mp}$ = Maximum voltage	(Parnis and Oldham, 2013)
4	Efficiency with active area	$\eta = \frac{A_S (J_{mp} V_{mp})}{A_C P_{IN}}$	$A_S$ = Effective illuminated area $A_C$ = Total geometric area	(Fritts and Fritts, 1883)
5	Fill factor	$FF = \frac{J_{mp} V_{mp}}{J_{SC} V_{OC}}$	$J_{SC}$ = Short-circuit current. $V_{OC}$ = Open-circuit voltage.	(Parnis and Oldham, 2013)
6	Beer-Lambert Law	$I(\lambda, x) = I_0(\lambda) e^{-\alpha(\lambda)x}$	$x$ = Thickness of the material $I(\lambda, x)$ = Intensity of light at $x$ $I_0(\lambda)$ = Initial intensity of light $\alpha(\lambda)$ = Absorption coefficient	(Aroutiounian et al., 2001)
7	Generation rate at a certain depth	$G(\lambda, x) = \alpha(\lambda) \phi_0(\lambda) [1 - R(\lambda)] \exp[-\alpha(\lambda)x]$	$G(\lambda, x)$ = Generation rate at $x$ $R(\lambda)$ = Reflection coefficient	(Rehman et al., 2023)

### 3. History and development of solar cells

Alexandre Edmund Becquerel invented the first photovoltaic cell in 1839 by coating platinum electrodes with silver chloride or silver bromide (Fonash, 2010). In 1882, the first practical photovoltaic (PV) cell using selenium as a photosensitive material was developed by Charles Fritts, however, it was costly with around 1% efficiency (Czochralski, 1918). In 1916, the Czochralski method was developed by the Polish chemist Jan Czochralski, which is a technique to grow single-crystal semiconductor materials (Chapin et al., 1954). The first practical crystalline silicon solar cell was developed using the Czochralski method in 1954 by a team of researchers at Bell Laboratories in the United States and the efficiency was around 6% (Loff, 2023). In 1958, solar cells became more significant with the addition of their use on the Vanguard-1 satellites, the first solar-powered satellite ever (Yamaguchi et al., 2021).

Throughout the years, the evolution of solar cells has marked numerous significant milestones, reflecting an unwavering commitment to enhancing efficiency and affordability. It began in the early days with the introduction of crystalline silicon cells and progressed to thin-film technology. The next century saw the development of organic and hybrid solar cells, as well as the exploration of new materials and nanotechnology. A notable advancement in solar technology is the use of tandem or multi-junction solar cells, which combine several materials for increased efficiency. Due to their efficiencies exceeding 40%, multi-junction (MJ) solar cells are gaining interest (Arumetha et al., 2017). Furthermore, perovskite solar cells emerged as true game-changers, showcasing rapid efficiency improvements and the potential for tandem configurations with traditional silicon cells. The solar business is actively adopting cutting-edge ideas and materials in the present environment to push efficiency limits and solve environmental issues.

### 4. Classification of solar cells

Solar cells can be categorized based on generations or materials. Most researchers sort solar cells by generations to show technological progress. However, there is no widely accepted method to classify third and fourth-generation solar cells, causing conflicts. To mitigate this conflict, we have chosen to classify cells based on their materials. The classification is demonstrated in the flowchart provided in Fig. 4.

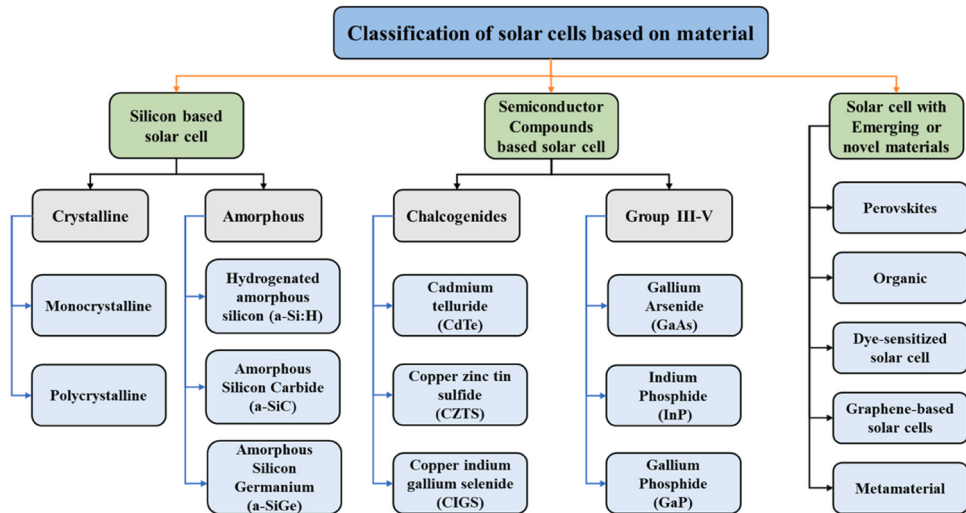


Fig. 4. Material-based classification of solar cells.

#### 4.1. Silicon-based solar cell

Silicon is the most extensively employed substance in photovoltaic cells. It is naturally abundant as silicon dioxide in sand and quartz, and it is extracted through carbon reduction techniques (Ferrazza, 2012). The manufacturing process involves purifying silicon, producing silicon blocks, slicing them into wafers, surface treatment, doping, and adding metal contacts (Wilson et al., 2020). Crystalline-silicon (c-Si) solar cells are the dominant and widely adopted due to their reliability, proven technology, and economies of scale (Philips et al., 2023). In 2021, the c-Si share of production in the photovoltaic market was around 95% of overall production. The mono-crystalline technique accounts for approximately 84% of total c-Si manufacturing (Anon, 2023b). Typical efficiency ranges of commercial poly-Si and mono-Si solar cells are around 15–17% and 20–23% respectively (Green, 1993). They have a long operational lifespan of 25–30 years or more, displaying excellent durability and stability.

Silicon solar cells have seen significant evolution over the years. In 1954, researchers at Bell Laboratories introduced the first modern silicon solar cell, initially using lithium diffusion for junction formation, which resulted in an efficiency of 4.5% (Loff, 2023). Later, the efficiency was raised by 6% when lithium was replaced by boron diffusion, and 10% efficiency was achieved by subsequent cell structural improvements (Mandelkorn et al., 1962). Initially, positive and negative connections were located at the back side of the cell. However, as cell design evolved, metal grids were introduced on the top surface. In the early 1960 s, efficiency exceeded 14% through a transition from phosphorus-doped substrates to boron-doped substrates. This shift required electrons to travel longer distances, taking advantage of their three-fold higher mobility compared to holes (Mandelkorn and Lamneck, 1973). In the 1970 s, it was found that adding alloyed aluminum to the cell's back side increased total electrical output. In 1972, Joseph Mandelkorn and John H. Lamneck Jr. introduced the concept of the 'back surface field' (BSF), which involved the addition of a heavily doped p-type layer at the rear surface using alloyed aluminum. The BSF is crucial in reducing minority carrier concentrations near the rear of the cell, limiting their transit to the rear contact. This is essential for lowering the effective minority carrier recombination velocity on the cell's back surface (Lindmayer and Allison, 1990). Furthermore, the implementation of a textured antireflection coating (ARC) on the top surface, along with photolithographically defined top contact fingers, resulted in an efficiency increase to 17% (Mandelkorn et al., 1962), (Green et al., 1986). Another significant improvement was achieved with the introduction of passivated emitter solar cells (PESCs), which

utilize a thin SiO<sub>2</sub> layer to passivate the non-contacted area of the top surface, thus preventing unwanted premature recombination. In 1985, an efficiency of approximately 20% was attained by incorporating a passivation layer on a highly boron-doped float zone silicon wafer (Ribeyron, 2017). The next significant advancement in cell design was the passivated emitter and rear contact (PERC) cells, which achieved an efficiency of 22% by adding a passivation layer in the back side. Furthermore, a 1% efficiency improvement was realized by locally diffusing both the top and bottom sides, resulting in a cell type known as passivated emitter, rear locally diffused (PERL) cell (Mandelkorn et al., 1962). In Fig. 5a, the configuration of a silicon solar cell used to get 25% efficiency is provided (Yoshikawa et al., 2017). In this design, both the emitter and the back contact were passivated by silicon oxide, while optical losses are reduced by a double-layer ARC and inverted pyramid microstructures. The cell structure of a silicon cell with a record efficiency of 26.3% is shown in Fig. 5b (Qarony et al., 2017). The Kaneka design makes use of interdigitated back contact (IBC) solar cells, in which the anode and cathode connections are arranged in an interdigitated pattern at the rear side of the cell. This design effectively eliminates shadowing losses caused by front-grid metallization, leading to increased efficiency, and optical losses were minimized by using an ARC on the top (Qarony et al., 2017).

Non-crystalline or amorphous (Fig. 5c) silicon is the semiconductor used in amorphous silicon (a-Si) solar cells. They are also referred to as thin-film silicon solar cells. Hydrogen is added to amorphous silicon in solar cells to passivate defects and dangling bonds, improving electronic properties and stabilizing the material. This process enhances carrier lifetime, reduces recombination, and optimizes optical absorption, contributing to increased efficiency and long-term performance in converting solar energy into electricity. The efficiency of a-Si:H solar cells typically ranges from 7% to 10%, and they are distinguishable from conventional crystalline silicon solar cells by their disordered atomic arrangement, which has a single crystal structure (Iddha et al., 2023). The highest efficiency of a-Si cell is found as 12.69%, which is provided in Table 2. The usual design of an a-Si:H solar cell is shown in Fig. 5d. In addition, the primary focus of research on the hydrogenated amorphous silicon germanium (a-SiGe:H) alloy is its narrow bandgap absorber function, to improve the stability of a-Si:H solar cells and the solar spectrum response at longer wavelengths (Yu et al., 2019a). Moreover, one study shows that with the ideal amount of Ge doping, the resulting radial junction a-Si:Ge alloy thin film solar cell exhibited remarkable electrical characteristics, achieving an efficiency of 6.26% (Hsu et al., 2019). Furthermore, hydrogenated amorphous silicon carbide (a-SiC:H) often used as a window layer in the silicon heterojunction (SHJ) solar

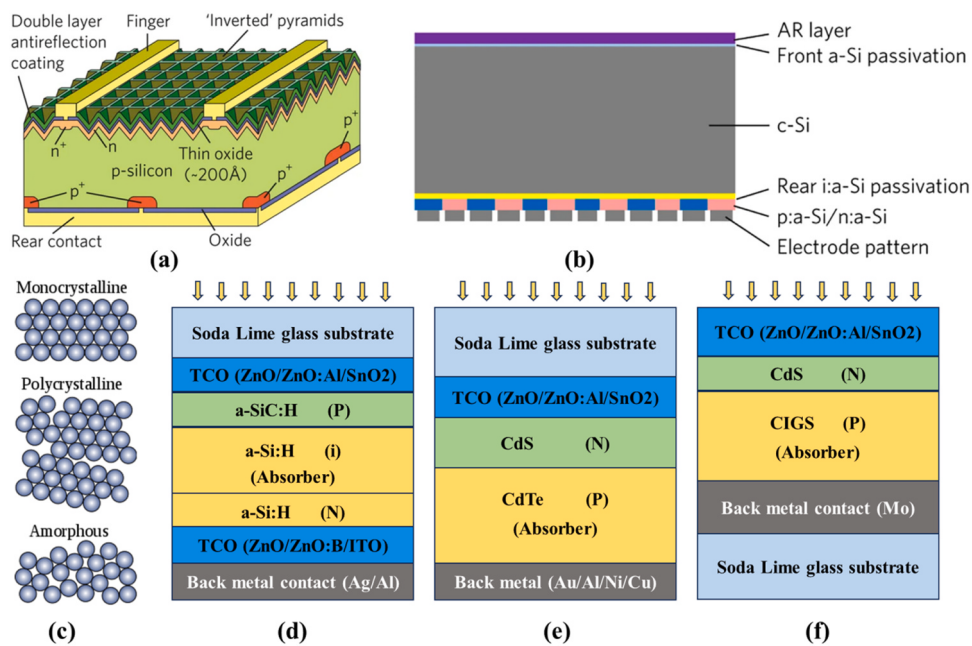


**Fig. 5.** a) Silicon solar cell design that achieves 25% efficiency (Yoshikawa et al., 2017). b) The setup for the 26.3% efficiency record (Qarony et al., 2017). c) Crystal Structure of mono-Si, poly-Si, and a-Si. Typical cell structure of d) a-Si, e) CdTe, and f) CIGS thin-film cell (Green, 2002). (Reused with permission. Copyright © 2017, Springer Nature).

**Table 2**

Single-junction and multi-junction terrestrial cell efficiencies were measured under the global AM1.5 spectrum ( $1000 \text{ W/m}^2$ ) at  $25^\circ\text{C}$ .

Classification	Efficiency (%)	V <sub>oc</sub> (V)	J <sub>sc</sub> (mA/cm <sup>2</sup> )	Fill factor (%)	Test center (date)	Description
Silicon-based solar cell						
Si (crystalline)	25	0.706	42.7	82.8	Sandia (3/99)	UNSW, p-type PERC (Matsui et al., 2015)
Si (crystalline)	26.7	0.738	42.65	84.9	AIST (3/17)	Kaneka, n-type rear IBC (Qarony et al., 2017)
Si (amorphous cell)	10.2	0.896	16.36	69.8	AIST (7/14)	AIST (Sai et al., 2018)
Si (microcrystalline cell)	11.9	0.550	28.72	75	AIST(2/17)	AIST (Green et al., 2023)
Group III-V material-based solar cell						
GaAs	29.1	1.1272	29.78	86.7	FhG-ISE (10/18)	Alta Devices (Anon, 2014)
InP	24.2	0.939	31.15	82.6	NREL (3/13)	NREL, crystalline cell (Zhu et al., 2022)
Chalcogenide compound-based solar cell						
CIGS	23.6	0.7671	38.30	80.5	FhG-ISE (1/23)	Evolar/UppsalaU (Anon, 2014)
CdTe	22.3	0.8985	31.69	78.9	NREL (2/23)	First Solar (Anon, 2014)
CZTS	11.4	0.7458	21.79	69.9	NPVM (5/23)	UNSW (Cd-free) (Anon, 2014)
Solar cell with emerging materials						
Perovskite	26	1.19	26	84	JET (3/23)	IoS/CAS (Anon, 2014)
Organic	19.2	0.9135	26.61	79	NREL (3/23)	SJTU (Ren et al., 2023)
Dye-sensitized	13	1.0396	15.55	80.4	FhG-ISE (10/20)	EPFL (Geisz et al., 2018)
Multijunction solar cell						
GaInP/GaAs (mqw)/GaInAs	39.5	2.997	15.44	85.3	NREL (9/21)	NREL, multiple QW (Anon, 2014)
5 junction cell (bonded) (2.17/1.68/1.40/1.06/.73 eV)	38.8	4.767	9.564	85.2	NREL (7/13)	Spectrolab, 2-terminal (Anon, 2014)
6 junction (monolithic) (2.19/1.76/1.45/1.19/.97/.7 eV)	39.2	5.549	8.457	83.5	NREL (11/18)	NREL, inv. Metamorphic (Lin et al., 2022)
Perovskite/Si	33.7	1.974	20.99	81.3	JRC/ESTI (5/23)	KAUST, 2-term (Anon, 2014)
Perovskite/perovskite	29.1	2.154	16.51	81.7	JET (12/22)	NanjingU/Renshine, 2-term (Chen et al., 2022)
Perovskite/organic	23.6	2.136	14.56	75.6	JET (3/22)	NUS/SERIS, 2-term (Shockley and Queisser, 1961)

cells (Ramanujam et al., 2020). Solar cells made of silicon have been cheaper over time, although they are still generally more expensive than certain newer technologies. Reducing costs and increasing efficiency is the goal of continuous research and development.

#### 4.2. Compound semiconductor-based solar cell

The unique electrical properties of compound semiconductor materials, which are made up of two or more elements from different periodic table groups, make them ideal for solar cell applications. In a solar cell, these substances could act as the active layer. Compound semiconductor-based PV cells have two aspects: group III-V

semiconductor-based solar cells and chalcogenide-based solar cells. Group III-V semiconductor-based solar cells use semiconductors made of elements from groups III (gallium, aluminum) and V (arsenic, phosphorus) of the periodic table. On the other hand, chalcogenide-based solar cells are made of materials that contain elements from the chalcogen group, which include sulfur (S), selenium (Se), and tellurium (Te). Thin-film solar cells mostly use materials like gallium arsenide (GaAs), cadmium telluride (CdTe), copper indium gallium selenide (CIGS), among others. These substances are applied to substrates like glass, metallic foils, and plastic sheets as thin layers (Moutinho et al., 1995). The manufacturing processes involve deposition techniques like physical vapor deposition (Kartopu et al., 2016) or chemical vapor

deposition (Anon, 2023c), enabling large-scale production and the creation of lightweight and flexible solar modules. Typically, cells made of chalcogenide materials have lower efficiencies compared to wafer-based silicon cells. For example, CdTe solar cells typically have an efficiency range of 9–11% (Green, 1993), although a recorded efficiency of 22.3% has been reported (Anon, 2023d). Fast Solar claims that its commercial module efficiency is approximately 18% (Anon, 2023d). CdTe is the only material that is affordable enough to rival crystalline silicon. Although silicon continues to dominate the photovoltaic industry, CdTe currently has a market share of about 5% (Anon, 2023b). Typically, CIGS solar cells have efficiency of 12–14% (Efazl et al., 2021). In terms of commercialized modules, the performance of CIGS is reported 19.2% (Adamovic et al., 2017). The typical structure of CdTe and CIGS are provided in Fig. 5(e & f). Thin-film solar cells offer flexibility and versatility in design, making them suitable for curved surfaces, building-integrated photovoltaic (BIPV) applications, and portable devices. Though they have increased their market share in a few specialized applications, such as BIPV and portable devices (Moon et al., 2019), first-generation silicon cells still dominate utility-scale installations.

#### 4.3. Solar cell with emerging or novel materials

Emerging solar cell technologies include novel methods, materials, and techniques in various phases of development, from early-stage research to near-commercialization. Their objective is to improve the efficiency, affordability, and adaptability of solar cells. Some can exceed the Shockley-Queisser limit, which is a significant gain over past solar cell generations in terms of materials, cost, and efficiency. The present target is to develop solar cells having energy conversion efficiency values double or triple the typical 15–20% range (Chopra et al., 2004). These solar cells' materials might be organic or nanostructured, and greater than 60% efficiency can be attained by employing various charge carrier collecting strategies (Kojima et al., 2009). The development of the charge carrier mechanism, charge collection, and energy harvesting in various new technologies have received more attention (Kojima et al., 2009). The following list includes some novel materials and cutting-edge technologies that have been studied in the context of solar cells.

##### 4.3.1. Perovskite solar cell

Halide perovskites, a group of materials, show promise for high-performance and cost-effective solar cells. The term "perovskite" stems from their crystal structure. Materials following the formula  $ABX_3$ , where X is an anion, and A and B are cations of varying sizes (with A being larger than B), are classified as perovskites. Perovskites' crystal structure is shown in Fig. 6b. In 2009, the organic-inorganic lead halide perovskite compounds  $\text{CH}_3\text{NH}_3\text{PbBr}_3$  and  $\text{CH}_3\text{NH}_3\text{PbI}_3$  were deposited as nanocrystalline particles on the  $\text{TiO}_2$  surface by Miyasaka and his

colleagues to study their photovoltaic properties.  $\text{CH}_3\text{NH}_3\text{PbBr}_3$  and  $\text{CH}_3\text{NH}_3\text{PbI}_3$  sensitized photovoltaic cells provided 3.13% and 3.81% efficiencies respectively (Anon, 2023e). Recent years have seen a dramatic development of perovskite solar cells, with efficiency rising from about 3% in 2009 to over 25% currently (Green et al., 2014). Rapid advancements in solid-state perovskite solar cells led to significant efficiency gains, in 2013 the efficiency was reported 16.2%, and 17.9% in early 2014 (Li et al., 2022). In 2022, a perovskite cell was fabricated based on  $\text{Cs}_{0.05}\text{FA}_{0.95}\text{PbI}_3$  composition (of  $1 \text{ cm}^2$ ) by using vacuum evaporation and the efficiency obtained was 23.44% for  $1 \text{ cm}^2$  aperture area (Hoppe and Sariciftci, 2004). In Fig. 6a, the schematic structure of a typical Planar Perovskite Solar Cell is provided.

##### 4.3.2. Organic photovoltaics (OPVs)

OPVs utilize organic materials or polymers to convert sunlight into electricity. Semiconducting organic materials' ability to conduct electricity and absorb UV-visible light is attributed to carbon atoms'  $sp^2$ -hybridization, leading to  $\pi$ -bond formation and dimerization in conducting polymers. The resulting delocalized  $\pi$ -electrons, influenced by the isomeric effect, contribute to significant electronic polarizability (Yin et al., 2016). Typically, organic solar cells are categorized into three groups according to their production method: Single-layer, Bilayer, and Bulk heterojunction organic cells. Three main components make up the basic structure of a single-layer organic solar cell. First, there is a modified transparent anode that lets light to pass through; these are commonly composed of materials like indium tin oxide (ITO). The second component is the active layer mix, which sits between the anode and the third one, a metal cathode with a low work-function that is frequently made of calcium (Ca) or aluminum (Al). Excitons are produced by the active layer when it is exposed to light. These excitons divide into electrons in the acceptor's lowest unoccupied molecular orbital (LUMO) and holes in the donor's highest occupied molecular orbital (HOMO) at the interface of the donor and acceptor. Then, after passing through the active layer, these charges are finally gathered by the matching opposing electrodes (Benanti and Venkataraman, 2006). Moreover, Bilayer heterojunction organic cells have an interface made of two materials with complimentary electronic characteristics. The donor layer, often a conjugated polymer, absorbs light and generates excitons, while the acceptor layer, often a fullerene derivative like C<sub>60</sub>, acts as an electron acceptor. This arrangement enhances exciton separation, charge mobility, and efficiency through a built-in electric field, enabling broader light absorption for improved power conversion (Lu et al., 2015). Bulk heterojunction organic cells involve blending donor and acceptor materials into a thin film with a dispersed interface, maximizing interfacial area and exciton diffusion. This enhances charge separation, reduces recombination losses, and promotes efficient charge collection through percolated pathways, resulting in superior power conversion compared to bilayer heterojunctions with restricted

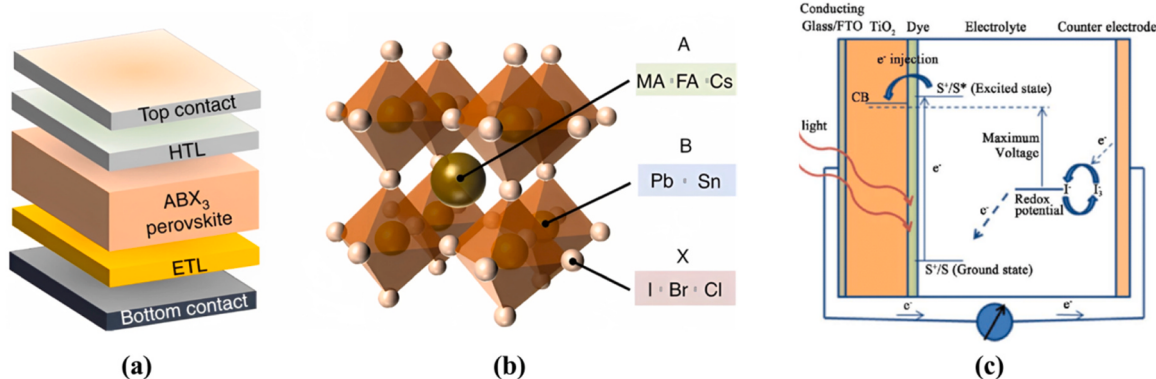


**Fig. 6.** a) Schematic structure of a typical Planar Perovskite Solar Cell, b) typically crystal structure of Perovskite material (Geim and Novoselov, 2007). c) design and operation of a dye-sensitized solar cell (Sharma et al., 2018). (Reused with permission. Copyright © 2022, Springer Nature).

interfaces (Cui et al., 2019). OPVs offer potential benefits such as low-cost manufacturing processes, flexibility, and the ability to be integrated into various surfaces. However, they are relatively less efficient and durable than conventional solar panels. Recent advances in OSCs demonstrated 16.5% efficiency in single-junction devices (Meng et al., 2018). For tandem devices, the efficiency is reported as 17.3% (Anon, 2023f). The efficiency of organic solar cells has significantly grown during the past few decades, reaching 19.2% (Chao et al., 2023). In 2023, Hyperbolic metamaterial (HMM) was applied in organic cells and the HMM-incorporated OSCs (HMM-OSCs) improved power conversion efficiency significantly (Grätzel, 2003).

#### 4.3.3. Dye-sensitized solar cells (DSSCs)

DSSCs require an electrolyte and a photoactive dye to absorb sunlight. Typically, four components are needed for DSSC to function: the photoanode, which is made of a semiconductor with high bandgap; the sensitizer, which serves as a photon collector; the electrolyte, which contains a pair of chemical substances for dye regeneration; and the counter-electrode (Sharma et al., 2018). A dye-sensitive solar cell's construction and functioning are shown in Fig. 6c. In a typical solar cell, silicon (Si) performs two jobs: it produces photoelectrons and creates an electric field that separates charges and produces current. While photoelectrons are produced by photosensitive dyes, the majority of the semiconductor in DSSCs primarily serves as a charge transporter (Bose et al., 2015). An interesting finding was presented in a review study by Bose et al., indicating that dye-based photovoltaic (PV) modules perform better at higher temperatures than Si-based modules, which perform worse (Çakar et al., 2022). The most frequently used substrates in DSSCs are TiO<sub>2</sub>, N719 dye, Iodide Ion (I<sup>-</sup>), Triiodide Ion (I<sub>3</sub><sup>-</sup>) and Platinum (Pt). TiO<sub>2</sub> is used as a photoanode, N719 ruthenium-based metal are used as dye, I<sub>3</sub>/I redox couple is involved in the electron transfer reactions, and Pt is used as a counter electrode (Kunzmann et al., 2018). In 1993, Grätzel et al. reported a cell efficiency of 9.6%, which increased to 10% at the NREL in 1997 (Bose et al., 2015). For N719 dye-based DSSC, 11.2% efficiency was reported in the review by Bose in 2015. A DSSC with a hybrid dye and titanium nanoparticle basis showed an efficiency of 8.75% in 2018 (Kakiage et al., 2015). For the DSSC constructed using Au/GNP as a counter electrode, Co<sup>3+/2+</sup> as a redox couple, and carboxy-anchor organic dye (LEG4) + alkoxysilyl-anchor dye (ADEKA-1) as a sensitizer, a maximum efficiency of 14.3% was mentioned (Ren et al., 2022). In October 2022, a group of scientists led by Grätzel fabricated DSSC with an efficiency of 15.2% (Zhou et al., 2022). DSSCs offer advantages such as low-cost materials,

environmental friendliness, flexible designs, and the ability to generate electricity in low-light conditions.

#### 4.4. Graphene-based solar cell

A significant focus is directed toward graphene (G), which holds the highest scientific and technological potential among nanomaterials. Graphene is a remarkable material composed of a 2D honeycomb lattice structure formed by closely packed carbon atoms. The hexagonal arrangement of the carbon atoms in this lattice gives it the appearance of a honeycomb. Presently, some researchers consider graphene as the fundamental building block of graphitic structures, leading to various allotropes with distinct dimensionalities, including 0D buckyball, 1D nanotubes, and 3D graphite, illustrated in Fig. 7(a-c) (Bonaccorso et al., 2010). The amazing optical and electrical characteristics of graphene, such as its high mobility, optical transparency, flexibility, and stability, are of great interest. Current research primarily centers on exploring fundamental physics and developing electronic devices utilizing these properties (Park et al., 2012). Due to its exceptional transparency and electrical conductivity, graphene is an excellent replacement for transparent conductive materials like indium tin oxide (ITO) (Fig. 7a-c) (Wang et al., 2008). For instance, in a dye-sensitized solar cell, graphene shows high conductivity of 550 S/cm and a transparency of more than 70% (over 1000–3000 nm) when the metal oxides window electrodes are replaced by graphene (Zhang et al., 2019). Moreover, the high electron mobility and superior charge transport capabilities of graphene can increase the collection of photogenerated electrons from the solar cell's active layer (Kumar et al., 2013). Positive charge carriers (holes) may be successfully extracted by a layer of graphene oxide (GO), while negative charge carriers (electrons) can be successfully extracted by a layer of graphene oxide that has been neutralized by cesium (GO-Cs). The total performance of the solar cell is enhanced by this tactical design, which maximizes the extraction of both types of charge carriers for improved energy conversion. Besides, solar cells can have graphene coatings applied to their surfaces to reduce reflection and boost light absorption. To minimize reflection losses, graphene's refractive index can be adjusted (Liu et al., 2012a).

Recent advancements in graphene-based solar cells increased their efficiency by roughly 20% by reducing incident light reflection (Loh et al., 2016). Graphene can be doped in different ways to enhance the efficiency. The only difference between graphene-based and inorganic solar cells is that graphene or materials derived from graphene replace inorganic components (Loh et al., 2016). In Fig. 7(d & e), general

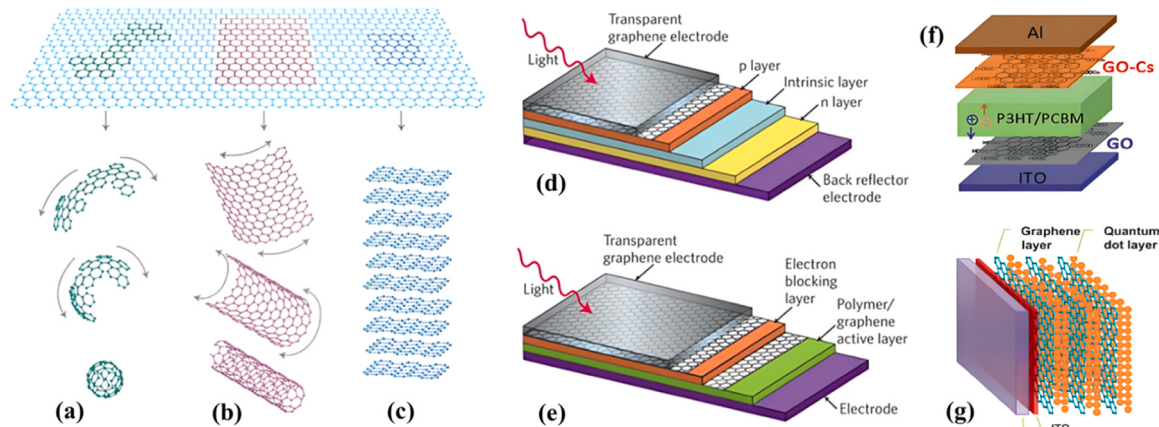


**Fig. 7.** Various layouts of honeycomb-like carbon atoms depending on their dimensionality. It can be coiled into a) zero-dimensional buckyballs, b) rolled into a one-dimensional nanotube or c) stacked into three-dimensional graphite (Bonaccorso et al., 2010) (reuse with the permission, Copyright © 2007, Springer Nature). Graphene-based d) inorganic, and e) organic solar cell (Park et al., 2012) (reuse with the permission, Copyright © 2010, Springer Nature). f) Device structures with GO and GO-Cs (Liu et al., 2012b) (reuse with the permission. Copyright © 2012, John Wiley and Sons). g) A stacked graphene-CdS quantum dot (QD) solar cell schematic (Iqbal et al., 2022) (reuse with the permission. Copyright © 2012, Springer Nature).

structures of graphene-based inorganic and organic solar cells are demonstrated. In addition, Graphene can be utilized as an intermediate layer between multiple solar cell materials in tandem cell designs (Chen et al., 2014). The total  $V_{OC}$  of a MJ solar cell is the sum of its subcell  $V_{OC}$ s. In tandem polymer solar cells, a GO/GO-Cs bilayer with extremely thin Al and MoO<sub>3</sub> can serve as an efficient connecting layer, significantly raising  $V_{OC}$  to over 100% of the total subcell  $V_{OC}$ s (Fig. 7f) (Wang et al., 2012). Further, solar cells made of inorganic quantum dots (QDs) may be able to go over the Shockley-Queisser limit, but their current limitations include low efficiency due to poor electron-hole separation and inadequate electron movement to electrodes (Iqbal et al., 2022). Guo et al. used graphene as a new electron acceptor to produce multi-layered graphene-QD QD solar cells. The device structure is illustrated in Fig. 7g.

#### 4.4.1. Metamaterial

Metamaterials are artificially engineered materials with unique properties that enable exceptional manipulation of electromagnetic waves. Their integration into solar cells has shown potential for enhancing light absorption and thus improving photovoltaic efficiency. Metamaterial-enhanced solar cells are actively researched for integration into various solar cell types, including conventional silicon cells, thin-film cells, and tandem cells, to improve photon absorption and enhance overall efficiency. Remember that this technology is still in its early stages of development (Abdulkarim et al., 2022). The development of a perfect metamaterial absorber (PMA) is an efficient method for enhancing the effectiveness of PV cells. Optical metamaterial-based perfect absorbers function in the optical or mid-infrared range, operating between 300 and 430 THz. These absorbers are promising for applications like solar cells and electromagnetic cloaking because they need unit cell size in the nanometer range, which is feasible using nanofabrication techniques (Hossain et al., 2023). The efficiency of solar cells made of perfect metamaterials can be increased by amplifying the solar waves that hit the PMA. From simulation research, the absorber's absorption rates for 549.20 THz and 653.2 THz were found to be 99.987% and 99.997%, respectively (Karami et al., 2021). The PMA structure consists of three layers, and the corresponding reflection and absorption spectrum are illustrated in Fig. 8a-b. In another work, a metamaterial absorber achieves almost complete absorption (more than 98%) over a wide field of view for mid-infrared wavelengths (1.77–4.81

$\mu\text{m}$ ). The absorber is constructed through a four-layer stack, employing a genetic algorithm to optimize the nanostructure array for broad bandwidth absorption, field-of-view, and polarization independence. Fig. 8 (c-d) shows the structure and absorptivity graph. Metamaterials can be engineered to capture a wider range of wavelengths which will allow solar cells to harvest more of the available solar energy. Moreover, Light can be trapped (Hamouche et al., 2017) and guided (Jing et al., 2020) by metamaterial structures inside the PV cell's absorber, enlarging its path and improving absorption. Jing et al. demonstrates through experimentation that metamaterial based on hybrid organic-inorganic perovskites (HOIP) can absorb visible light and show up to 40% greater photocurrent than flat films (Bossard et al., 2014).

The light trapping ability of broadband metamaterial perfect absorbers (BMMPA) can be used in solar thermophotovoltaics (STPVs). STPV is a conversion method that uses photonic reemission to convert heat into electricity, as depicted in Fig. 8e. BMMPA can be used to increase the absorption of STPVs because it has broadband absorption capabilities. A lot of research has been done on STPV systems since theoretical models predict up to 85% efficiency (Dincer et al., 2014). Efficient solar thermophotovoltaic (STPV) systems require absorbers that achieve broad-spectrum absorption from ultraviolet to near-infrared while minimizing energy loss due to mid-infrared thermal radiation, being angle and polarization-independent. There has been a lot of interest in the development of improved BMMPAs, which use square rings with four gaps to give polarization angle independence for solar applications throughout microwave, infrared, and visible wavelengths (Li et al., 2014). Tungsten, molybdenum, and tantalum are favored refractory metals due to their high melting points, although they lack optimal absorption in the visible range. In one material study by researchers, titanium nitride (TiN), has shown its potential for use in STPVs with an average absorption rate of 95% over the 400–800 nm wavelength range (Güney et al., 2009). The challenge in solar thermophotovoltaic (STPV) and metamaterial (MM) solar cell systems lies in maintaining stability under high temperatures and intense light exposure, which are essential for practical operation. Efficiency can be hindered by Ohmic loss and material heating caused by strong currents in metallic nanostructures. Researchers propose geometric modifications, such as increasing corner radius, to mitigate these losses (Green, 2015). Yu et al. proposed the "bulk skin depth technique" to shift optical absorption from metallic structures to semiconductors, reducing Joule

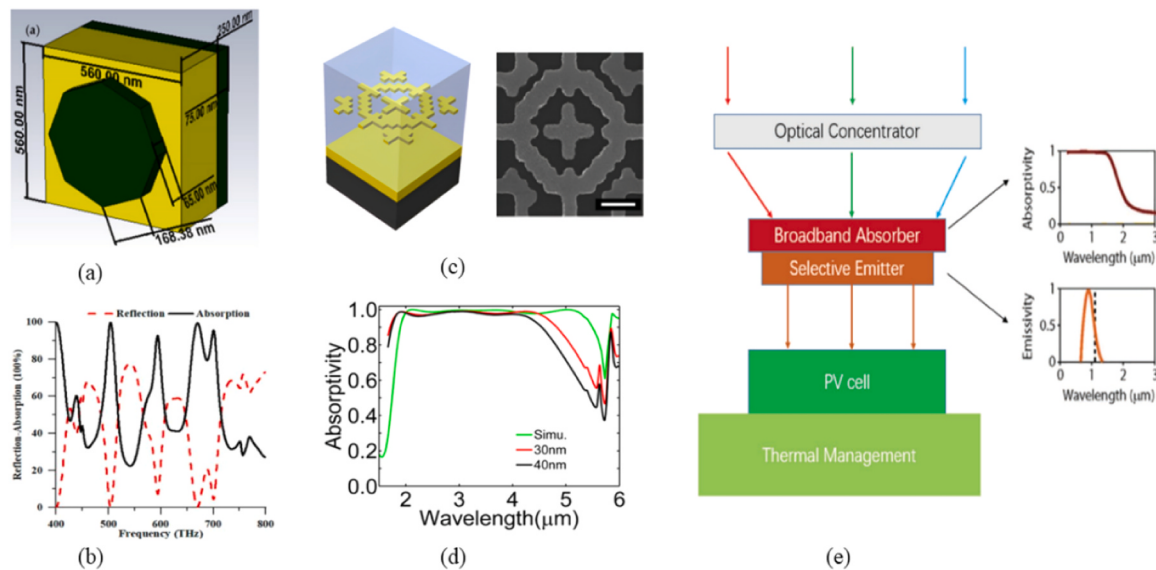


Fig. 8. a) Schematic diagram of PMA and b) corresponding reflection and absorption spectrum (Karami et al., 2021). c) Schematic of the Pd-based PMA structure (left). FESEM image of one unit cell (right). d) Simulation and measurements for Pd nanostructure thicknesses of 30 and 40 nm (Yu et al., 2019b). e) Schematic of STPV systems (Fraas et al., 2003) (reuse with the permission. Copyright © 2018, John Wiley and Sons).

heating and enabling additional interconnections without damaging the absorber (Fraas et al., 2003).

## 5. Different types of losses in solar cell

The power conversion efficiency of a solar cell is a parameter that quantifies the proportion of incident power converted into electricity. The Shockley-Queisser (SQ) model sets an upper limit on the conversion efficiency for a single-gap cell. According to this model, a single-gap cell can achieve 30% conversion efficiency when the bandgap is 1.1 eV (Kumar and Kumar, 2017). However, achieving this limit in practice is challenging due to various losses and limitations in real-world solar cell devices, as the SQ limit is a theoretical calculation based on the principles of thermodynamics and detailed balance (Kumar and Kumar, 2017). Charge carrier collecting efficiency, charge carrier separation efficiency, thermodynamic efficiency, and conductive efficiency are some of the components that constitute cell efficiency (Kim et al., 2016). The sum of these separate efficiencies yields the total efficiency.

The amount of incident solar energy that is transformed into electrical power in photovoltaic systems is rather minimal. The vast majority of lost energy is utilized to heat-up equipment, which raises the temperature and inescapably lowers the effectiveness of solar devices (Wang and Xuan, 2018). Losses in solar cells can result from a variety of physical and electrical processes, which have an impact on the system's overall functionality and power conversion efficiency. These losses may happen during the solar cell's light absorption, charge creation, charge collecting, and electrical output processes, among others. Two types of solar cell losses can be distinguished: intrinsic and extrinsic losses (Hirst and Ekins-Daukes, 2011). The flowchart provided in Fig. 9 demonstrates individual components of Intrinsic and extrinsic losses. Table 4 describes different formulas related to different losses of a solar cell.

### 5.1. Intrinsic losses

Intrinsic losses are the basic losses that occur in solar cells. Even with ideal solar cells, intrinsic losses in single bandgap cells are unavoidable. Below  $E_g$ , thermalization, emission, angle mismatch, Carnot, and angle mismatch are five loss processes that can be used to categorize as intrinsic losses (Dupré et al., 2016). Fig. 10a. shows the p-n junction's conversion losses in a typical setting. These losses can be rapidly sketched using a dual-axis diagram (Fig. 10c).  $E_g/q$  indicates the maximum voltage ( $V_{max}$ ) that can develop in the cell. When all incoming photons with higher energy than  $E_g$  are fully absorbed and contribute to the current, the maximum current density ( $J_{max}$ ) is attained. It has been demonstrated that intrinsic loss mechanisms and power out depend on  $E_g$  (Fig. 10b) and the number of junctions (Fig. 10d). In Table 3. The fraction of all the intrinsic losses is provided.

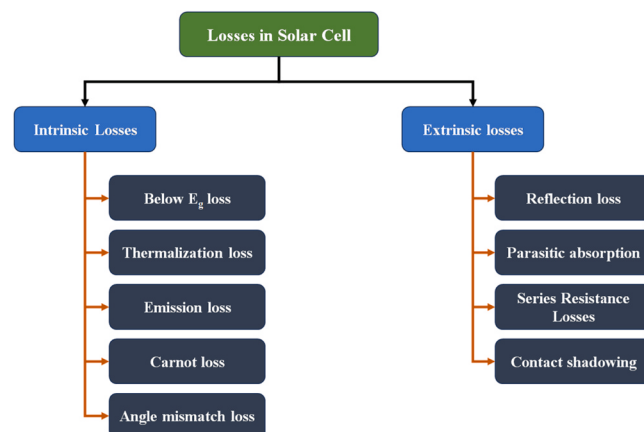


Fig. 9. Different types of losses in solar cells.

Table 3

The fraction of incident light attributed to different loss mechanisms for a cell under one sun illumination (with  $E_g = 1.31$  eV).

Mechanism	Percentage (%)
Power out	32.5
Below-bandgap ( $E_g$ ) loss	25
Thermalization loss	29.8
Carnot loss	2.2
Boltzmann loss	9.3
Emission loss	1.1

It can be observed that, the impact of below  $E_g$  loss and thermalization loss are significant among others.

#### 5.1.1. Below $E_g$ loss

Photons with energies below the bandgap remain unabsorbed in a solar cell due to the mismatch between the broad solar spectrum and the specific energy absorption characteristic of a single bandgap ( $E_g$ ) (Dupré et al., 2016). Due to incident photons' inability to be reflected and insufficient energy to excite an electron over the band gap, this loss takes place. The lattice atoms, free carriers, or rear metallization can either let these photons escape the cell or absorb them. If the photons are taken in, their energy is converted to phonons, which are the material's lattice vibrational quanta, and this adds to the heat source (Hirst and Ekins-Daukes, 2011). The associated power loss due to "Below  $E_g$  loss" can be calculated using Equation 8.

#### 5.1.2. Thermalization loss

Photovoltaic equipment has a particular kind of energy loss called thermalization loss. In a solar cell, excited electrical carriers with extra energy are produced when a semiconductor material absorbs light. In order to reach their thermal equilibrium distribution, these carriers rapidly relax toward the band edges, losing a portion of their energy in the process. This process happens very quickly, in about  $10^{-12}$  seconds (Garner and Garner, 1979). Heat is produced when the extra energy is transferred to the phonons, which are the lattice vibrational quanta in the material. Equation 9 can be used to compute the corresponding heat source as a result of thermalization loss.

#### 5.1.3. Emission loss

According to Kirchoff's law, materials that absorb light must also emit light, and this emission from the solar cell contributes to a decrease in conversion efficiency (Dupré et al., 2016). The loss of photons emitted by the cell due to radiative recombination is known as emission loss. This rate of photon emission is directly related to the bias voltage ( $V$ ) and can be determined using Rau's reciprocity principle (Garner and Garner, 1979). The emission loss can be expressed by Equation 10.

#### 5.1.4. Carnot loss

The Carnot loss relates to the theoretical maximum limit on the efficiency of a solar cell, stemming from the temperature difference between the cell and its surrounding environment. This limitation arises from the Carnot efficiency, which is determined by the temperature contrast between the heat source and the heat sink and applies to various heat engines. In the context of a solar cell, the solar cell itself serves as the heat source, heated by absorbed sunlight, while the surrounding environment represents the heat sink at a lower temperature (Dupré et al., 2016). This process also generates associated heat, which can be represented by Equation 11.

#### 5.1.5. Angle mismatch loss

When sunlight strikes a solar cell at an angle other than the ideal angle, there is a voltage reduction known as an angle mismatch loss. At the point where the air and solar cell meet, light is refracted and reflected, causing this loss. Equation 12 can be used to determine the heat generation due to angle mismatch (Hirst and Ekins-Daukes, 2011).

**Table 4**  
Formulas for different loss mechanisms.

Equation no.	Parameter	Formula	Nomenclature	Ref.
8	Below $E_g$ loss	$P_{Below} = n \int_0^{E_g} (1 - R_c - T_c) PFD(E) \cdot E dE$	$P_{Below}$ = The below $E_g$ loss $E_g$ = Bandgap of the material $n$ = Concentration ratio of the cells (n suns) $R_c$ = Reflectance of the cell $T_c$ = Transmittance of the cell $E$ = Photon energy $PFD(E)$ = Photon flux density	(Hirst and Ekins-Daukes, 2011)
9	Thermalization loss	$P_{Thermalization} = n \int_{E_g}^{\infty} (1 - R_c - T_c) PFD(E) \cdot (E - E_g) dE$	$P_{Thermalization}$ = Thermalization loss $(E - E_g)$ = Surplus energy of photons with energy over the bandgap	(Garner and Garner, 1979)
10	Emission loss	$P_{Emission} = E_g \int_{E_g}^{\infty} n(E, T_a, qV_c, \Omega_e) dE$	$P_{Emission}$ = Emission loss $T_a$ = Temperature of the cell $V_c$ = Voltage across the cell $\Omega_e$ = Solid angle of emission	(Dupré et al., 2016)
11	Carnot loss	$P_{Carnot} = J \Delta V_{Carnot}$	$P_{Carnot}$ = Carnot loss $J$ = Output photocurrent of the cell $\Delta V_{Carnot}$ = Voltage loss associated with Carnot efficiency in a thermodynamic system	(Hirst and Ekins-Daukes, 2011)
12	Angle mismatch loss	$P_{Angle} = J \Delta V_{Angle}$	$P_{Angle}$ = Angle mismatch loss $\Delta V_{Angle}$ = Voltage loss due to unbalanced solid angles of absorption and emission	(Hirst and Ekins-Daukes, 2011)
13	Reflection loss	$P_{reflection} = \int_0^{\infty} R(E) PFD(E) E dE$	$P_{reflection}$ = Reflection loss $R(E)$ = Spectral reflectance of the device	(Garner and Garner, 1979)

## 5.2. Extrinsic losses in solar cells

Extrinsic losses in solar cells are typically attributable to outside forces or circumstances that are unrelated to the material characteristics or underlying physical principles of the solar cell. These elements include issues like contact shadowing, parasitic absorption, reflection loss, and series resistance (Hirst and Ekins-Daukes, 2011), (Abdullah et al., 2016). Although they have the potential to drastically reduce the device's efficiency, these losses are theoretically avoidable, hence they are not taken into account when determining the fundamental limiting efficiency.

### 5.2.1. Reflection loss

The amount of solar radiation energy reflected by the device can have a substantial influence on this loss, which affects the efficiency of the solar cell as a whole. The typical loss of incident light from reflection from a silicon solar cell's front surface is 30%, which lowers the efficiency of the device's total power conversion (Wang et al., 2017). The reflection loss can be expressed as Equation 13.

### 5.2.2. Parasitic absorption

Parasitic absorption refers to the absorption of light in non-active layers or materials within a solar cell that is not intended for efficient charge generation. Transparent conductive layers, contact layers, anti-reflection coatings, and passivation layers can all contribute to parasitic absorption losses (Fell et al., 2022). While these layers serve important functions in the solar cell, they may also exhibit some degree of light absorption, reducing the available light for conversion into electricity. Efficiency losses in the solar cell result from parasitic absorption, in which absorbed light does not help produce charge carriers. Addressing and reducing parasitic absorption is necessary to increase the overall efficiency and performance of solar cells (Werner et al., 2016a). Through a low-temperature bleaching procedure incorporating CO<sub>2</sub> plasma treatment, parasitic absorption within the transparent electrode can be reduced (Pysch et al., 2007).

### 5.2.3. Series resistance losses

Series resistance is a key factor in efficiency decrease in solar cells. It includes the total resistance that the current encounters as it flows through the semiconductor material, conductive layers, and in-

terconnections of the solar cell. This resistance limits the available effective voltage to drive the current, resulting in power and efficiency losses. Solar cells with a surface area of 15.6 × 15.6 cm<sup>2</sup> can generate currents of up to 8.2 A (Servaites et al., 2010). Longer metal fingers are a result of expanding solar cell sizes. As a result, there is an increase in power loss that is attributed to greater currents and longer fingers increasing series resistance. Therefore, it is unquestionably crucial to reduce series resistance as much as feasible. In organic photovoltaic cells, series resistance can be optimized by developing new active layer materials that can increase the active layer mobilities (Gupta et al., 2015).

### 5.2.4. Contact shadowing

Contact shadowing is a solar cell phenomenon brought on by the existence of electrical contacts or conductive fingers on the cell's surface, which throw shadows and block incoming sunlight. These shadows lower the amount of light that reaches the active photovoltaic material, causing localized power production reductions and decreased efficiency (Fathi et al., 2017). Moreover, hotspots are created on photovoltaic panels due to the shading effects of the metal grid. When a hotspot arises, the temperature in the affected region can rapidly rise, causing thermal stress and potentially panel melting. This might harm the panel permanently and reduce its overall efficiency. Furthermore, hotspots can reduce the output voltage of the panel, lowering its performance even further (Sarkin et al., 2020).

## 6. Efficiency improvement methods of solar cell

The ability of solar cells to convert sunlight into electricity is directly impacted by their efficiency, making it a crucial component of solar cell technology. Utilizing the sun spectrum and implementing efficient light management techniques can increase the efficiency of solar cells.

### 6.1. Light management

Effective light management is an essential component in the design of PV cells to increase light absorption and boost the overall efficiency of photovoltaic systems. Efficient light management strategies include Anti-Reflection Coatings (Jošt et al., 2017), Texturing (Hsiao et al., 2012), Plasmonic Nanoparticles (Curtin et al., 2009), and Back

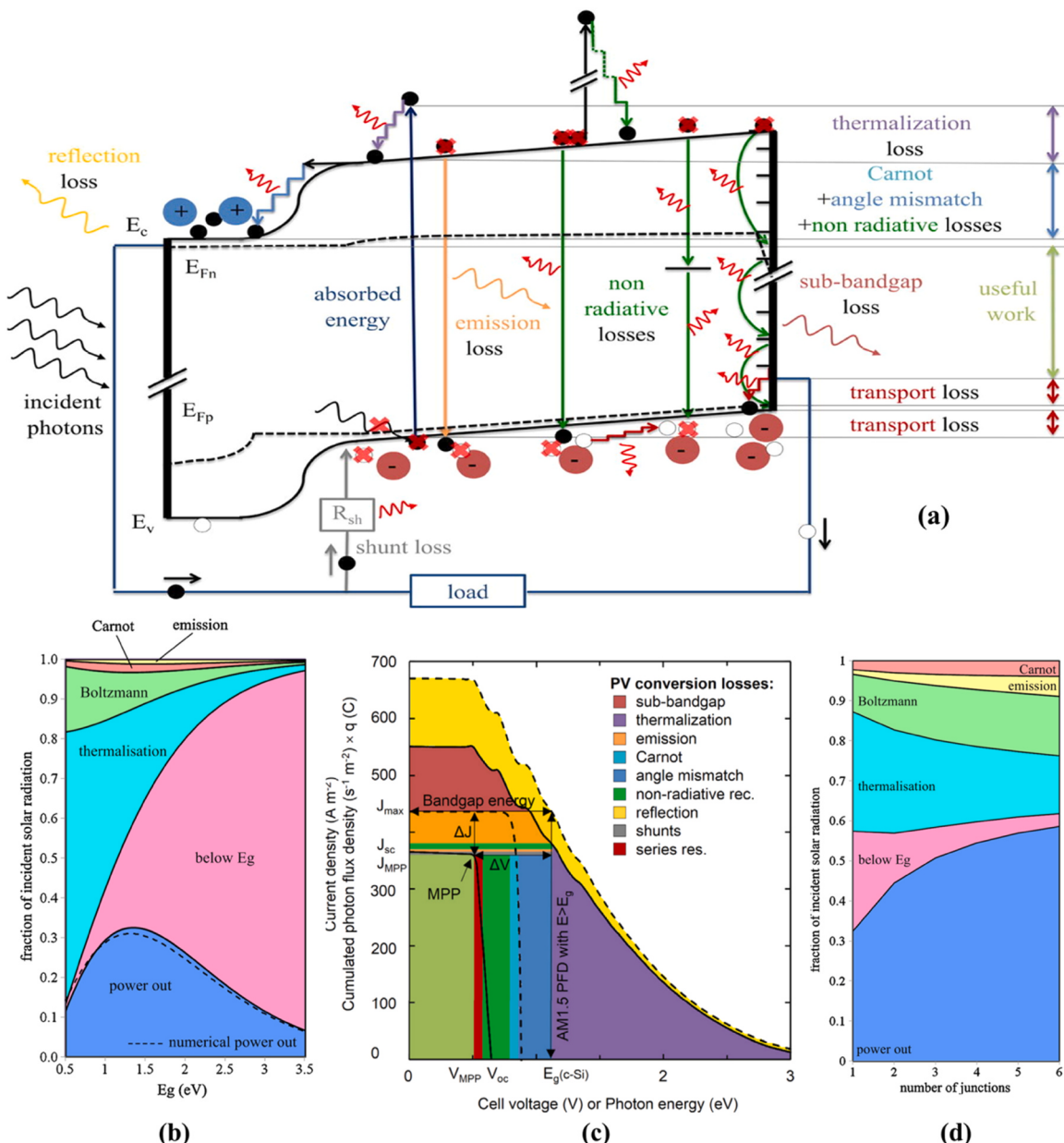


**Fig. 10.** a) Typical single junction PV cell's P-n Junction diagram showing the processes of energy conversion loss (Garner and Garner, 1979). b) It is demonstrated that intrinsic loss mechanisms and power out depend on  $E_g$  (Dupré et al., 2016). c) A c-Si solar cell's current density as a function of voltage and photon flux density times electrical elementary charge as a function of photon energy (Garner and Garner, 1979). d) Intrinsic loss mechanisms and power out depending on the number of junctions (Dupré et al., 2016). (reuse with the permission. Copyright © 2016, Elsevier, and Copyright © 2010, John Wiley and Sons).

Reflectors (Addie et al., 2022). These techniques aim to capture a significant amount of sunlight, increase photon absorption in the active semiconductor material, and reduce losses due to reflection and transmission.

Solar cells' surfaces are coated with anti-reflection coatings (ARCs) to reduce the reflection of incoming light. Fig. 11h illustrates how this decrease in reflection losses permits more light to enter the solar cell's active area, improving light absorption and total efficiency. Amorphous carbon nitride ( $CN_x$ ) thin layer was used as an ARC in crystalline silicon (c-Si) solar cells in recent research, which led to an increase in efficiency from 5.52% to 13.05% (Forberich et al., 2008). Another study found that covering organic solar cells with moth eye anti-reflection material boosted their efficiency by 3.5% (Sahouane and Zerga, 2014). Multi-layer ARC can be used to increase efficiency even more (Papet et al., 2006).

Surface texturization, several micro/nanoscale textures on surfaces,

is used to boost the efficiency of solar cells. As shown in Fig. 11i, this method increases light transmission while decreasing reflection at interfaces, which is crucial for improving the efficiency of solar cells' ability to convert sunlight into energy. Microstructures such as pyramids (Cho et al., 2013), 1D V-groove arrays (Li et al., 2015), and micro-groove lens structures (Moulin et al., 2011) can be used to increase light trapping and improve optical path length. Additionally, using a back reflector can increase the likelihood that the solar cell will be able to absorb light. A rear reflector is positioned after the absorber layer of a solar cell and is typically made of materials like  $ZnO/Ag$  or  $SiO_2/Ag$ . Its function is to reflect light that travels through the absorber layer and re-direct it into the cell (Kim et al., 2020). The use of Lambertian surface texture in solar cells randomizes light propagation, scattering light to the absorber, and utilizing back reflection to increase optical path length, enhancing photon absorption rates (de Aberasturi et al., 2015).

In solar cells, nanostructures are used for both the active layers and

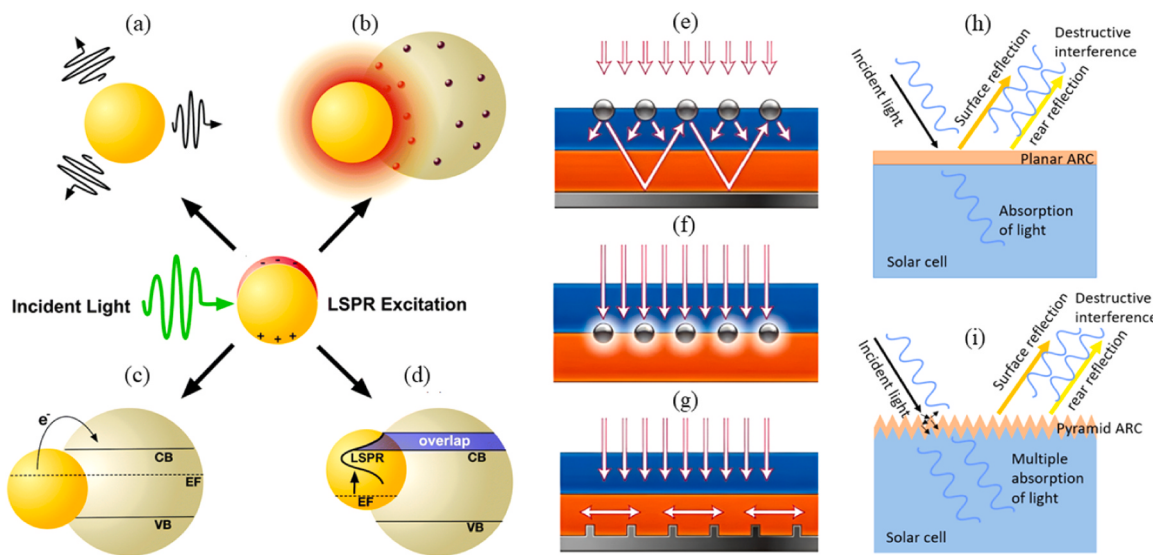


**Fig. 11.** A diagram of the plasmon enhancement mechanisms (Matheu et al., 2008) shows radiative effects like (a) far-field scattering and (b) near-field coupling as well as nonradiative effects like (c) hot-electron transfer and (d) plasmon resonant energy transfer. Three strategies for capturing light in thin-film solar cells using metallic plasmonic nanostructures (Zambree et al., 2023). (e) Metallic nanoparticles' impact on a cell, results in the scattering effect and angular redistribution of the scattered light. (f) implanted metallic nanoparticles' near-field effect. (g) metal nanostructures on the back contact are used to couple sunlight into SPPs. h) More light enters the cell because ARC reduces reflection. i) A textured surface gives a second chance for some of the reflected light to enter the cell (Stan et al., 2008). (Reuse with the permission. Copyright © 2010, Springer Nature).

light-management techniques (Erwin et al., 2016). Plasmonic enhancement in solar cells involves two key mechanisms. Firstly, radiative effects, driven by the relaxation of localized surface plasmon resonances (LSPR), lead to the re-emission of light into the absorbing layer, thereby amplifying local electric fields. This enhancement encompasses light scattering and electromagnetic near-field enhancement (Matheu et al., 2008). Secondly, non-radiative effects, also associated with LSPR relaxation, focus on transferring energy to nearby semiconductors, which significantly boosts current generation within the solar cell. These non-radiative effects encompass processes like hot electron transfer and plasmon resonant energy transfer (Matheu et al., 2008). In summary, plasmonic enhancement employs radiative effects to intensify local electric fields and re-emit light, while non-radiative effects involve energy transfer to neighboring semiconductors, ultimately enhancing the overall current production in solar cells. In Fig. 11(a-d) these mechanisms are shown. Plasmonics has been extensively studied for improving solar cells, both theoretically and experimentally. Plasmonic nanostructures can be used in three different ways: on the front surface (as shown in Fig. 11e) (Pfeiffer et al., 2014), integrated into the absorber (illustrated in Fig. 11f) (Prabhathan and Murukeshan, 2016), or at the lower interface (as shown in Fig. 11g) (Beck et al., 2009). Plasmonic nanoparticles, typically made of gold or silver, can scatter incident light, increasing its path length within the solar cell and enhancing absorption. The solar cell material's targeted absorption range may be matched to the nanoparticles' plasmon resonance, enhancing the absorption of particular wavelengths (Atwater and Polman, 2010). Plasmonic nanoparticles can also concentrate light into subwavelength volumes, beneficial for thin-film solar cells with limited absorption (Zambree et al., 2023). By integrating plasmonic nanoparticles, solar cells aim to optimize light management, increase absorption, reduce reflection losses, and improve efficiency.

## 6.2. Spectral utilization

Utilizing the complete solar spectrum effectively to increase cell efficiency is known as spectrum utilization in solar cells. The goal of this technique is to match the semiconductor material's absorption characteristics with the diverse solar spectrum, which includes wavelengths

from ultraviolet (UV) through infrared (IR). Effective spectral utilization can be achieved by using a variety of methods, such as multiple junctions, intermediate band gaps, quantum dot spectral converters, luminescent down-shifting (LDS) layers, and up-conversion materials. Solar cell efficiency could be considerably increased by improving spectrum utilization.

Multi-junction (MJ) solar cell is a very promising technique for attaining outstanding sunlight-to-electricity conversion efficiency. These cells are more effective because they employ a variety of absorber materials with different bandgaps, allowing them to effectively absorb a wider range of sunlight wavelengths and so enhance both spectrum utilization and overall efficiency. In 2008, a GaInP/GaAs/GaInAs triple-junction solar cell with better spectrum splitting achieved roughly 33% efficiency over a GaInP/GaAs/Ge 3 J cell (Philipps et al., 2018). A record efficiency of 39.2% can be obtained by using a six-layer multi-junction solar cell under AM 1.5 (Anon, 2014). In 2016, MJ concentrator solar cells made of III-V semiconductors reached more than 46% efficiency (McKenna and Evans, 2017). Currently, the recorded efficiency of a six-junction concentrator cell is found as 47.1% (Chao et al., 2023). The record efficiencies of different multi-junction solar cells are provided in Table 2. Therefore, by using materials with appropriate bandgaps for different parts of the solar spectrum (e.g., visible, infrared), a greater percentage of the sunlight spectrum may be used by MJ solar cells, converting more sunlight into electricity.

To increase the efficiency of single-junction solar cells by lowering thermalization and non-absorption losses, researchers are looking into the usage of luminescent materials as spectrum converters. Up-conversion, quantum-cutting, and down-shifting are three luminescence mechanisms that are being studied (Van Der Ende et al., 2009). Researchers concentrate on using trivalent lanthanide ions because of their intricate energy-level structure (referred to as the Dieke diagram), which permits efficient photon manipulation and spectral conversion (Huang et al., 2012). Following the Stokes Law for wavelength change, a high-energy photon is changed into a lower-energy photon during the single photon downshifting process (as depicted in Fig. 12a-left). While downshifting and quantum cutting are comparable, downshifting has a little lower conversion efficiency (Zhang and Huang, 2010). A conversion efficiency of more than 100% can be attained using quantum

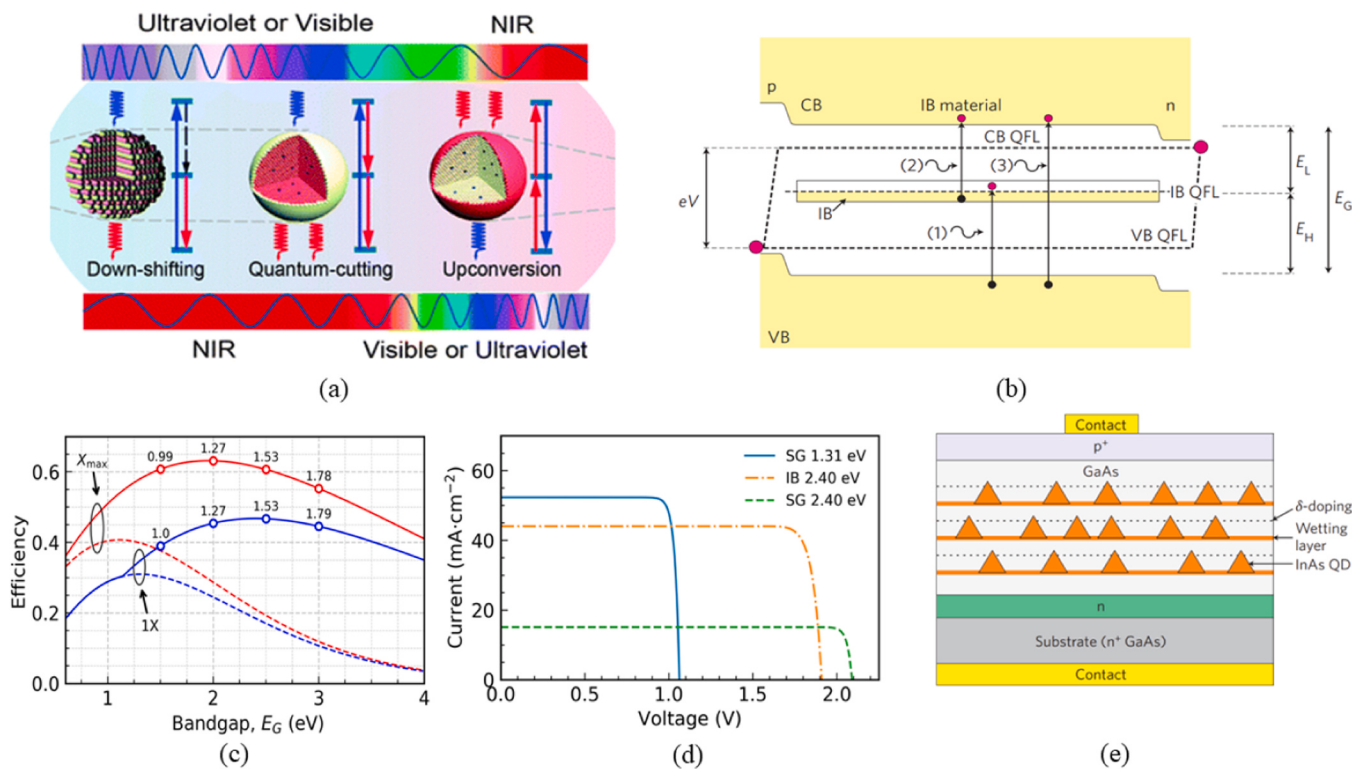


**Fig. 12.** a) Typical processes of down-shifting (DS), quantum-cutting (QC), and up-conversion (UC) using luminescent materials are shown (Zhang and Huang, 2010). b) Band diagram of an IB solar cell (Popescu et al., 2008). c) The diagram shows the efficiency of an ideal single-gap solar cell and an ideal intermediate-band solar cell based on the energy bandgap ( $E_G$ ). d) J-V curve of cells with single gap material of 1.31 eV and 2.40 eV, and an ideal Intermediate Band Solar Cell (IBSC) (Luque et al., 2012). e) Schematic of a QD IB solar cell (Popescu et al., 2008). (Reuse with the permission. Copyright © 2012, Springer Nature and Copyright © 2020, John Wiley and Sons).

cutting, as shown in Fig. 12a (middle). One incoming high-energy photon is split into two or more incoming photons of lesser energy to achieve this. The thermalization of hot charge carriers after the absorption of high-energy photons may cause energy losses, which may be mitigated by this process (Wang et al., 2010). The process of transforming two or more low-energy pump photons into a higher-energy output photon, as seen in Fig. 12a-right, is known as up-conversion in nonlinear anti-Stokes optics. In up-conversion, the upconverter converts several sub-bandgap photons into a single above-bandgap photon. This higher-energy photon may be absorbed by the solar cell, resulting in the formation of electron-hole pairs (Ramiro and Martí, 2021).

Intermediate band solar cells (IBSCs) are created with an extra energy level within the bandgap to use low-energy photons, as shown in Fig. 12b. This additional energy level enables the absorption of lower-energy photons. Under conditions of maximum solar concentration (46,050 suns), the IBSC provides 63% efficiency with only one semiconductor material (Fig. 12c) (Luque et al., 2012). An intermediate band (IB) material is sandwiched between two typical N-type and P-type semiconductors that function as selective contacts to the conduction and valence bands (CB and VB). These newly added energy levels make it easier for lower-energy photons to be absorbed, which eventually improves the efficiency of the entire conversion process. Photons with energy below the bandgap can be absorbed by the material at transitions from the VB to the IB and from the IB to the CB. The current produced by regular photons absorbed during the VB-CB transition is explained by these coupled transitions. The optimum bandgap of an ideal intermediate band (IB) solar cell is around 1.95 eV (under maximum concentration), and the IB divides it into two sub-bandgaps of about 0.71 eV and 1.24 eV (Popescu et al., 2008). At one sun, however, the efficiency is more than 40% for the ideal bandgap of 2.40 eV.

In Fig. 12d, ideal Single-Gap Solar Cells (SGSC) and ideal Intermediate Band Solar Cells (IBSC) operating under one sun are shown

together with their current-voltage (J-V) properties. The IBSC displays a little lower photogenerated current than the ideal SGSC, but a higher voltage, leading to a greater output power overall (Luque et al., 2012). Engineers have created experimental IBSC devices using quantum dot technology (Luque et al., 2004). In 2004, the first solar cells of this type were developed. The InAs quantum dots used in these cells, seen in Fig. 12e was generated using molecular beam epitaxy in the Stranski-Krastanov growth mode (Luque and Martí, 2001).

In 2001, Luque et al. proposed an alternative approach known as the 'Bulk with deep-level impurities (DLIs) (Marsen et al., 2012). This method involves creating an intermediate band by introducing deep levels through impurities in a host material. In 2003, Marsen et al. developed an IBSC of this type by using  $\text{CuGa}_{1-x}\text{Fe}_x\text{S}_2$  thin films as absorber materials (Yu et al., 2003). The addition of iron (Fe) within the  $\text{CuGaS}_2$  material led to the observation of light absorption at sub-gap energy levels (1.2 eV and 1.9 eV). Two other methods were proposed to develop IBSC: Highly mismatched alloys (HMAs) and Organic molecules (OMs). In HMAs, a slight addition of a new element to the primary material alters one of the bands of the main material. After then, this band divides into  $E_+$  and  $E_-$ . The intermediate band (IB) is defined as the lower-energy portion ( $E_-$ ) (Ekins-Daukes and Schmidt, 2008). In OM's method, photons of lower energy are absorbed by sensitizers in organic molecules, which then transmit that energy to a high-bandgap acceptor. The mechanism achieves upconversion through a sequence of phases involving triplet states and triplet-triplet annihilation (Anon, 2023g). Although each method in IBSC has progressed experimentally, none of the IBSC techniques completely utilizes the advantages of the intermediate band. While each approach has advantages and disadvantages, Quantum Dots have demonstrated the most anticipated phenomena in the operation of Intermediate Band Solar Cells (Luque et al., 2012).

By optimizing the spectral utilization of a solar cell, it becomes capable of efficiently absorbing a larger fraction of the solar spectrum.

This maximizes the conversion of sunlight into electrical energy and leads to higher overall efficiency. Different approaches, such as broad absorption characteristics, multi-junction designs, intermediate band concepts, and spectral conversion techniques, can be employed to enhance spectral utilization and improve solar cell efficiency.

## 7. Challenges, prospects, and future direction

### 7.1. Challenges exist in different types of solar cells

Solar cells can be categorized into different types based on the mechanisms they employ to convert sunlight into electricity. Each type presents unique challenges, and the following sections discuss the challenges and prospects of various kinds of solar cells.

#### 7.1.1. Silicon solar cells

Due to their high energy efficiency, silicon wafers have a 90% market share in solar cells, but the price to build these panels is higher than the alternatives (Smith et al., 2014). In c-si cells, thick wafers are used, which increases material costs. Silicon solar cells have a limited ability to capture low-energy photons, which limits their efficiency, especially in low-light conditions. Moreover, the practical limits in obtaining maximum efficiency are restricted by many factors including different types of recombinations and losses (Shah et al., 2004). Using thin-film silicon solar cells can reduce the material cost than classical wafer-based solar cells (Akimov et al., 2009). However, this will reduce the efficiency as well. Using nanotechnology (Dubey et al., 2014), distributed bragg reflector (DBR) (Peters et al., 2012), and introducing grating structure (Trompoukis et al., 2012) can enhance the efficiency of the thin-film silicon solar cell. Moreover, with cutting-edge manufacturing processes like nanoimprinting (Zhu et al., 2011) and laser doping (Roesch et al., 2015), silicon solar cells' efficiency can be improved.

#### 7.1.2. Compound semiconductor solar cells

The majority of chalcogenide compound semiconductor materials are utilized in thin-film solar cells. These materials can degrade over time due to environmental factors (Lin and Ravindra, 2020), affecting long-term performance and reliability (Nardone and Albin, 2015). Nardone and Albin examined two degradation mechanisms in CdTe solar cells: one attributed to defect generation in the interdiffusion region, and the other associated with an increase in the back barrier height, potentially arising from the out-diffusion of copper (Yang et al., 2020). Besides, Yang et al. investigate the strain-dependent impact on the power degradation of CIGS thin-film solar cells (Abermann, 2013). Furthermore, certain thin-film materials contain toxic elements, such as cadmium, raising environmental and disposal concerns (Romeo and Artegiani, 2021). CdTe solar cells have achieved efficiency beyond 22%, but their full potential lies in attaining higher voltage ( $V_{OC}$ ) and fill factor (FF) (Sites and Pan, 2007). To increase the open circuit voltage of the CdTe solar cell the net charge density and lifetime of the carrier should be increased (Theelen and Daume, 2016). Degradation of CIGS solar cells is mainly associated with reduced fill factor and open circuit voltage. Open circuit voltage is predominantly affected by changes in the absorber and pn-junction qualities, whereas the fill factor is mostly influenced by the introduction of alternate shunt routes and higher series resistance. One important tactic to stop degradation is to implement an effective water barrier inside the module. This will restrict the rise in ZnO:Al resistivity and maybe the molybdenum back contact, which will stop the series resistance from rising as seen (Liu et al., 2020). Efficacious p-type doping, passivation of defects, and investigation of alternate window layers are issues that must be resolved to further increase performance (Galagan, 2020).

#### 7.1.3. Perovskite solar cells

Perovskite solar cells must overcome particular technological

constraints to become a competitive commercial technology. Stability and durability, module effectiveness with scalability constraints, and manufacturing issues, including yield and process control, are the three basic categories into which these difficulties can be divided. The most serious technological concern for perovskite PV is its durability. In addition, some perovskite formulations may contain lead, raising concerns about their environmental impact and safe disposal. Moreover, it is difficult to move perovskite solar cells from low-volume laboratory production to high-volume manufacturing while maintaining performance (Sun et al., 2023). In recent research, it was found that these types of cells can retain approximately 80% of their initial efficiency after 600 h of operation under ambient conditions (Sieglar et al., 2022). Perovskite PV must last at least 20 years for leveled cost of electricity (LCOE) measures to reach the Solar Energy Technologies Office's (SETO) 2030 goals of \$0.02/kWh (Weerasinghe et al., 2015). Encapsulation (Zhao et al., 2021a), ion migration control (Wang et al., 2016), and the improvement of the intrinsic stability (Ma et al., 2022) of the perovskite absorber layer are some techniques to improve the stability of perovskite solar cell. The effect of encapsulation on perovskite-based solar cells is investigated by Weerasinghe et al (Zhao et al., 2021a). In addition, current encapsulation materials and strategies to commercialize perovskite solar cells are summarized by Ma et al (Tan et al., 2020). Apart from that, manipulating the size mismatch of the mixed "A" site composition (perovskite structure is  $ABX_3$ ) stops ions from moving around too much, increasing the stability of the solar cells (Sherafatipour et al., 2019).

#### 7.1.4. Organic solar cells

Organic solar cells (OSCs) are less efficient than their inorganic counterparts, which prevents a wide range of commercial applications. In addition, their sensitivity to oxygen and moisture shortens their lifespan and contributes to disintegration (Solak and Irmak, 2023). Because of specialized processing and performance uncertainty, large-scale production is difficult. Moreover, this type of solar cell has a shorter lifespan (typically around 10–15 years) compared to other cell technologies (Chen, 2019). Besides, the performance of OSC is studied in controlled lab environments, however, these devices will work in a variety of real-world conditions, including diverse atmospheres, indoor lighting, high illumination, and even underwater. There is a question if the performance of OSC will be the same or not. Apart from that, distribution, manufacturing, and material production are all part of the complex supply chain for OPV cells. Any interruption, such as shortages of components or materials, might have an impact on their price and availability (Chen, 2019). On the other hand, improvements to active-layer packaging and structure have been made to extend their lifespan and counter degradation processes. Additionally, the strategic removal of electron acceptors near the top electrode has enabled highly durable OSCs that remain functional underwater without encapsulation (Rahman et al., 2017).

### 7.2. Performance of silicon PV modules in extreme environmental condition

Although the photovoltaic (PV) module is capable of efficiently capturing solar radiation, the received irradiation may be reduced by man-made or natural barriers like dust, snow, or shadows. In addition, dust and other contaminants are absorbed by humid air, causing damage to the module and a decrease in incident light. When the PV panel is exposed to direct sunshine, it becomes heated. Light absorption by non-solar cell components also adds to module heating, which lowers bandgap energy and produces less power than is ideal. Many studies have examined the variables affecting the performance of PV modules. Temperature, dust accumulation, soiling, wind, shading, and humidity are among the environmental factors that have a major impact on efficiency.

### 7.2.1. Effect of temperature and strategies to overcome

The efficiency of a PV module is significantly influenced by its temperature. The efficiency of the module reduces with increasing temperature. Just 20% of solar energy is converted into electricity; the remaining 80% is converted into heat (Katkara et al., 2011). Literature indicates that at a cell temperature of 36°C, efficiency somewhat increases by up to 12%. However, efficiency starts to decrease above this temperature, as Fig. 13a illustrates. There are many efficient methods for controlling the operating temperature of solar cells which include both active and passive approaches. Active cooling relies on liquid or gas, along with fans and pumps, to dissipate extra heat. In contrast, passive cooling enhances convective heat transfer to the atmosphere by utilizing materials with high thermal conductivity or altered surface structures. Maintaining the maximum power production from PV modules requires the application of these strategies. The most common cooling methods are described in Table 5.

### 7.2.2. Effects of dust accumulation and strategies to overcome

PV module efficiency decreases when air contaminants such as dust, water vapor, and molecules in the air block sunlight from reaching the PV panel (Fig. 13b). Bigger dust particles scatter light, which reduces solar energy. Accumulation of dust on the module's surface can alter its optical characteristics, increasing light reflection from the front surface while reducing transmissibility and light absorption, all of which impact the output of the PV module. According to studies conducted in Saudi Arabia, the average monthly rate of efficiency deterioration is 6–7%, and without cleaning, it may rise to 13% in just six weeks. Moreover, the lack of cleaning may cause output power generation to drastically decrease, reaching only 50% of its peak value (Elnozahy et al., 2015). There are many cleaning processes investigated by PV researchers and some of the most promising cleaning methods are summarized in Table 6.

### 7.3. Future direction

The prospects of various solar cell technologies are promising but differ in focus. Silicon-based solar cells continue to evolve, with prospects for improved efficiency and cost reduction through advanced materials and manufacturing techniques. Introducing plasmonic nanoparticles and photonic crystals are promising methods to increase absorption in thin-film silicon cells (Bermel et al., 2007), (Snaith, 2013). Perovskite solar cells offer rapid efficiency gains, low-cost manufacturing, and versatility, positioning them for widespread

adoption (Werner et al., 2016b). Perovskite/silicon tandem solar cell shows a promising future and more work should be done in this area (Lal et al., 2017), (Al-Ashouri et al., 2020). In one study, a monolithic perovskite/silicon tandem cell shows around 29% efficiency even after 300 h of operation (Raza and Ahmad, 2022). Future efforts must prioritize addressing challenges like instability and material toxicity to successfully develop and commercialize c-Si/perovskite thin film solar cells (Noh et al., 2020).

Moreover, the prospects of inverse design in solar cell applications are exceptionally promising. Inverse design in the context of solar cells refers to a computational approach that aims to optimize the structure and properties of a solar cell by working backward from desired performance characteristics rather than relying solely on traditional trial-and-error methods. Recent advancements in materials science have shifted towards machine-enabled inverse design approaches, which leverage data-driven techniques such as high-throughput screening, global optimization, and generative models to expedite the discovery of advanced materials with predefined properties (Yu et al., 2013). Additionally, a copper-based thin-film PV absorber material has been found using an inverse design technique (Lu et al., 2022). Hybrid-organic-inorganic-perovskite (HOIP) solar cells have demonstrated impressive performance, but the search for environmentally friendly, lead-free alternatives with suitable bandgaps remains crucial for commercialization [223]. Inverse design can also apply to multi-junction solar cells to determine optimal materials, layer thicknesses, and parameters to achieve specific desired performance characteristics. Unlike traditional methods that start with available materials, inverse design begins with desired performance metrics and employs optimization algorithms or machine learning to find the necessary parameters.

## 8. Conclusion

The continuous evolution of solar cell technology has witnessed numerous novel technological advancements. Extensive research has been conducted on the progress of various solar cell technologies. Some review papers have focused solely on efficiency improvement methods. This study encompasses the current status of photovoltaic technology, reviewed loss mechanisms, efficiency improvement methods, and the challenges faced by different cell technologies and materials. The findings from this study are outlined as follows:

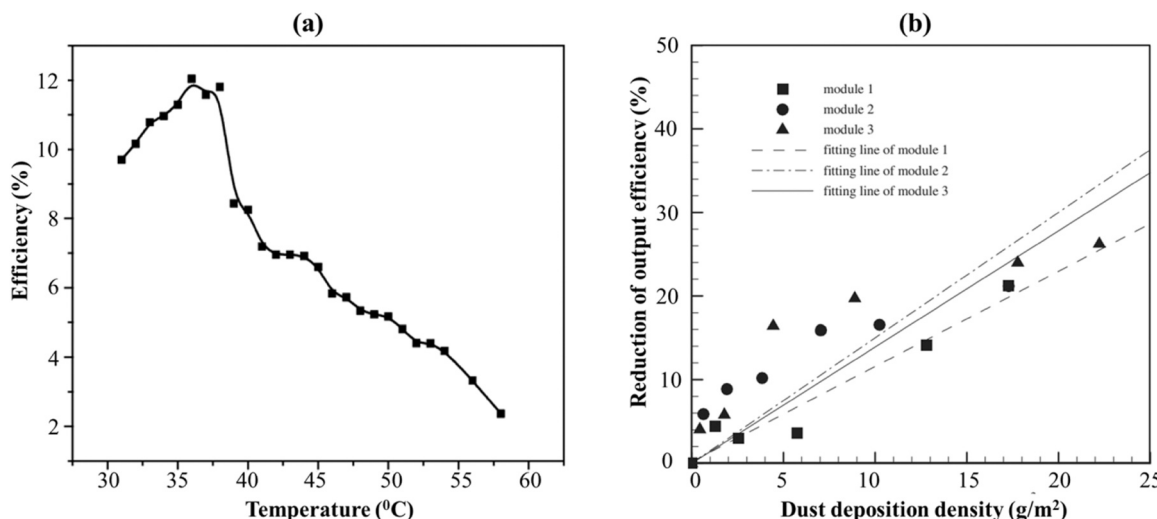


**Fig. 13.** a) Effect of temperature (Jiang et al., 2011), and b) dust deposition on module efficiency (Abdolzadeh and Ameri, 2009). (Reuse with the permission. Copyright © 2011, Elsevier).

**Table 5**

Different temperature control methods and experimental results.

Method	Description	Experiments	Result	Ref.
Direct spraying	Spray water directly on PV modules through sprinklers.	Directly sprayed water on PV modules in extreme weather.	Efficiency increased up to 3.26%	(Elbreki et al., 2021)
Increasing the fin's surface area	The fins are the expanded section that makes thermal contact with the PV module to absorb heat.	Used a planar reflector and lapped fins as part of a passive cooling technique.	The temperature difference between the reference PV module and the mean PV module was 24.6°C	s(Al Tarabsheh et al., 2016)
Coupled with thermal system	Cell temperature can be reduced by using a combined system.	Increased the PV performance by using a modified air-cooled PVT system.	The thermal efficiency was in between 15%–31% and the electrical efficiency was in between 12%–12.4%	(Choubineh et al., 2019)
Heat pipe technologies	The pipe absorbs the temperature of the module	Applied water and air cooling to the solar panel using a unique micro heat pipe arrangement.	The efficiency of the air and water cooling systems improved by 8.4% and 13.9%, respectively	(Hachem et al., 2017)
Phase change materials (PCM)	Phase change materials serve as latent heat storage materials, capable of absorbing excess heat	Investigated how employing pure and blended PCM affected a PV panel's electrical performance and thermal behavior.	For pure PCM, the electrical efficiency increased by 3%, while for combined PCM, it climbed by 5.8%	(Benghanem et al., 2016)
Thermoelectric cooling (TEC)	Thermoelectric cooling is a technology that utilizes the Peltier effect, using electric current to create a temperature gradient for heating or cooling purposes.	Tested solar cell performance in Madinah utilizing a thermoelectric cooling system	Efficiency increases by 0.5% per °C decrease in temperature	(Hasan et al., 2022)

**Table 6**

Promising cleaning methods and experimental results.

Method	Description	Experiment	Result	Ref.
Water cleaning	Requires a substantial volume of water under continuous high-pressure	Compared the performance of two modules: one cleaned and another one uncleansed	The cleaned module achieved an efficiency of 11.7%, whereas the uncleansed module exhibited a 9% efficiency	(Al Shehri et al., 2017)
Manual cleaning	Special bristle brushes are used to clear dust particles.	Evaluated several brush materials, including silicon rubber foam, nylon, and cloth	Utilizing silicone rubber for cleaning enhances the maximum power output by 1% compared to unbrushed panels	(Mani and Pillai, 2010)
Mechanical cleaning	An automated and mechanical water cleaning method	Cleaned and cooled the PV module using a robotic water spray	Efficiency increases by 15%	(Zhao et al., 2021b)
Electro-dynamic screens (EDS)	An electro-dynamic screen (EDS) can clean the module automatically	Compared the effect of the mechanical cleaning method and electrostatic coating	EDS eliminates more than 90% of dust in less than two minutes, making it useful in dry, arid, and desert environments.	(Assi et al., 2012)
Forced air-flow cleaning	Removing the dust using forceful airflow	Suggested a technique to cool and clean the module in the harsh United Arab Emirates (UAE) climate.	Used the forced air flow generated by cooled return air from air conditioning systems to eliminate the dust	(Zhi and Zhang, 2018)
Self-cleaning material	Materials used enable the water-repelling (hydrophobic) or water-dispersing (hydrophilic) qualities of the module	A superhydrophobic surface coating with strong antireflective qualities was created for potential application on solar cell glass covers.	The superhydrophobic coating demonstrated exceptional qualities of self-cleaning.	(Liu et al., 2019)

- The efficiency of silicon (Si)-based solar cells has nearly reached its maximum capacity at approximately 25%. Conversely, III-V compound semiconductor-based solar cells have consistently exhibited enhancements in performance, increasing by approximately 1% annually. These solar cells recently accomplished a remarkable efficiency of 47.1%. However, a major barrier to the widespread commercial viability of III-V solar cells is the high costs associated with them.
- Thin film solar cells are favorable due to their minimal material usage and increasing efficiency. Cadmium telluride (CdTe), copper indium gallium selenide (CIGS), and amorphous silicon ( $\alpha$ -Si) are the three main materials used in thin film solar cells. CIGS and CdTe solar cell technologies rival crystalline solar cells, the recorded efficiency of CIGS and CdTe solar cells are 23.6% and 22.3%, respectively. On the other hand, Perovskite solar cells demonstrate remarkable efficiency, reaching 26% for single junction and 33.7% for perovskite/silicon double junction cells. Environmental issues, the low open-circuit voltage of CdTe solar cells, and stability concerns for perovskite solar cells still persist.
- After reviewing the fundamental losses of single-junction solar cells, it was shown that thermalization loss and below-bandgap ( $E_g$ ) loss have a major impact. The below-bandgap loss is about 25% and the

thermalization loss is about 29.8% for a material having a bandgap of 1.31 eV.

- The integration of plasmonic nanoparticles onto the cell's surface offers encouraging opportunities for light trapping, whereas multi-junction solar cells demonstrate remarkable outcomes in terms of spectrum utilization.

With the potential to alter conventional wafer-based solar cells, future efforts must focus on resolving issues like instability and material toxicity to effectively develop and commercialize c-Si/perovskite thin-film solar cells. Additionally, researchers should strive to incorporate metamaterials into the solar cell to enhance light absorption, ultimately improving its efficiency.

## Funding

No funding support was available for this research.

## CRediT authorship contribution statement

**Abu S. M. Mohsin:** Writing – review & editing, Writing – original draft, Validation, Supervision, Resources, Project administration, Methodology, Investigation, Funding acquisition, Conceptualization.

**Md. Mosaddequr:** Writing – review & editing, Validation, Supervision, Resources, Project administration, Funding acquisition, Conceptualization. **Belal Bhuiyan:** Writing – review & editing, Validation, Supervision, Resources, Project administration, Funding acquisition, Conceptualization. **Atib Mohammad Oni:** Writing – original draft, Visualization, Validation, Methodology, Investigation, Formal analysis.

## Declaration of Competing Interest

The authors declare that they have no known competing financial interests or personal relationships that could have appeared to influence the work reported in this paper.

## Data Availability

No data was used for the research described in the article.

## Acknowledgment

Authors would like to thank Brac University for the research support.

### Author contribution

The author Atib Mohammad Oni<sup>1</sup> contributed to literature review and preparation of the manuscript. The author Abu S. M. Mohsin<sup>2</sup> contributed to conception of the paper, manuscript preparation and supervision. The authors Md. Mosaddequr Rahman<sup>3</sup>, and Mohammed Belal Hossain Bhuiyan<sup>4</sup> contributed to manuscript revision and supervision

## Disclosures

The authors declare no conflicts of interest.

## Appendix A. Supporting information

Supplementary data associated with this article can be found in the online version at [doi:10.1016/j.egyr.2024.03.007](https://doi.org/10.1016/j.egyr.2024.03.007).

## References

- Liu, L., 2009. “Comment on ‘recent progress in thermodynamics of radiation-exergy of radiation, effective temperature of photon and entropy constant of photon,’ (Jun.). Sci. China, Ser. E: Technol. Sci. vol. 52 (6), 1809–1810. <https://doi.org/10.1007/S11431-009-0086-4>/METRICS.
- Shah, A.S.B.M., Yokoyama, H., Kakimoto, N., 2015. High-precision forecasting model of solar irradiance based on grid point value data analysis for an efficient photovoltaic system (Apr.). IEEE Trans. Sustain Energy vol. 6 (2), 474–481. <https://doi.org/10.1109/TSTE.2014.2383398>.
- Anon. “International Technology Roadmap for Photovoltaic: Publication of the 14th edition - vdma.org - VDMA.” Accessed: Aug. 08, 2023a. [Online]. Available: <https://www.vdma.org/viewer/-/v2article/render/78984725>.
- D. Feldman, K. Dummit, J. Zuboy, and R. Margolis, “Summer 2023 Solar Industry Update,” 2023a.
- Haegel, N.M., et al., 2023. Photovoltaics at multi-terawatt scale: waiting is not an option (Apr.). Science (1979) vol. 380 (6640), 39–42. <https://doi.org/10.1126/SCIENCE.ADF6957>.
- Anon.“Crystalline Silicon Photovoltaics Research | Department of Energy.” Accessed: Sep. 14, 2023b. [Online]. Available: <https://www.energy.gov/eere/solar/crystalline-silicon-photovoltaics-research>.
- Carlson, D.E., Wronski, C.R., 1976. Amorphous silicon solar cell (Jun.). Appl. Phys. Lett. vol. 28 (11), 671–673. <https://doi.org/10.1063/1.88617>.
- Böer, K.W., 2011. Cadmium sulfide enhances solar cell efficiency (Jan.). Energy Convers. Manag. vol. 52 (1), 426–430. <https://doi.org/10.1016/J.ENCONMAN.2010.07.017>.
- Chu, T.L., Chu, S.S., 1993. Recent progress in thin-film cadmium telluride solar cells (Jan.). Prog. Photovolt.: Res. Appl. vol. 1 (1), 31–42. <https://doi.org/10.1002/PIP.4670010105>.
- Rezaei, N., Procé, P., Simor, M., Vroon, Z., Zeman, M., Isabella, O., 2020. Interdigitated back-contacted structure: A different approach towards high-efficiency ultrathin copper indium gallium (di)selenide solar cells (Sep.). Prog. Photovolt.: Res. Appl. vol. 28 (9), 899–908. <https://doi.org/10.1002/PIP.3296>.
- Jaiswal, R., Kumar, A., Yadav, A., 2022. Nanomaterials based solar cells (Jan.). Nanotechnol. Automot. Ind. 467–484. <https://doi.org/10.1016/B978-0-323-90524-4.00025-6>.
- Kamat, P.V., 2013. “Quantum dot solar cells (Mar.). big thing Photovolt.,” J. Phys. Chem. Lett. vol. 4 (6), 908–918. [https://doi.org/10.1021/JZ400052E/ASSET/IMAGES/MEDIUM/JZ-2013-00052E\\_0013.GIF](https://doi.org/10.1021/JZ400052E/ASSET/IMAGES/MEDIUM/JZ-2013-00052E_0013.GIF).
- Sharma, K., Sharma, V., Sharma, S.S., 2018. Dye-sensitized solar cells: fundamentals and current status. Nanoscale Res Lett. vol. 13 <https://doi.org/10.1186/S11671-018-2760-6>.
- Servaites, J.D., Ratner, M.A., Marks, T.J., 2011. Organic solar cells:a new look at traditional models (Oct.). Energy Environ. Sci. vol. 4 (11), 4410–4422. <https://doi.org/10.1039/C1EE01663F>.
- Anon, “Renewables 2022 – Analysis - IEA.” Accessed: Aug. 30, 2023a. [Online]. Available: <https://www.iea.org/reports/renewables-2022>.
- D. Feldman, K. Dummit, J. Zuboy, and R. Margolis, “Spring 2023 Solar Industry Update,” 2023b.
- M. Woodhouse et al., “Research and Development Priorities to Advance Solar Photovoltaic Lifecycle Costs and Performance,” 2021, Accessed: Sep. 12, 2023. [Online]. Available: [www.nrel.gov/publications](http://www.nrel.gov/publications).
- Righini, G.C., Enrichi, F., 2020. Solar cells’ evolution and perspectives: a short review (Jan.). Sol. Cells Light Manag.: Mater., Strateg. Sustain. 1–32. <https://doi.org/10.1016/B978-0-08-102762-2.00001-X>.
- Roy, P., Kumar Sinha, N., Tiwari, S., Khare, A., 2020. A review on perovskite solar cells: Evolution of architecture, fabrication techniques, commercialization issues and status (Mar.). Sol. Energy vol. 198, 665–688. <https://doi.org/10.1016/J.SOLENER.2020.01.080>.
- Asim, N., et al., 2012. A review on the role of materials science in solar cells (Oct.). Renew. Sustain. Energy Rev. vol. 16 (8), 5834–5847. <https://doi.org/10.1016/J.RSER.2012.06.004>.
- Haug, F.J., Ballif, C., 2015. Light management in thin film silicon solar cells (Mar.). Energy Environ. Sci. vol. 8 (3), 824–837. <https://doi.org/10.1039/C4EE03346A>.
- Schmid, M., 2017. Review on light management by nanostructures in chalcopyrite solar cells (Mar.). Semicond. Sci. Technol. vol. 32 (4), 043003. <https://doi.org/10.1088/1361-6641/AA59EE>.
- Berry, F., et al., 2022. Light management in perovskite photovoltaic solar cells: a perspective (May). Adv. Energy Mater. vol. 12 (20), 2200505. <https://doi.org/10.1002/AENM.202200505>.
- Baiju, A., Yarema, M., 2022. “Status and challenges of multi-junction solar cell technology.” (Sep.). Front Energy Res vol. 10, 971918. <https://doi.org/10.3389/FENR.2022.971918>/BIBTEX.
- Siah Chehreh Ghadikolaei, S., 2021. Solar photovoltaic cells performance improvement by cooling technology: an overall review (Mar.). Int. J. Hydrol. Energy vol. 46 (18), 10939–10972. <https://doi.org/10.1016/J.IJHYDENE.2020.12.164>.
- Anon, 2002. Solar radiation at the top of the atmosphere (Jan.). Int. Geophys. vol. 84 (C), 37–64. [https://doi.org/10.1016/S0074-6142\(02\)80017-1](https://doi.org/10.1016/S0074-6142(02)80017-1).
- Green, M.A., 2012a. Limiting photovoltaic efficiency under new ASTM International G173-based reference spectra (Dec.). Prog. Photovolt.: Res. Appl. vol. 20 (8), 954–959. <https://doi.org/10.1002/PIP.1156>.
- Green, M.A., 2012b. Limiting photovoltaic efficiency under new ASTM International G173-based reference spectra (Dec.). Prog. Photovolt.: Res. Appl. vol. 20 (8), 954–959. <https://doi.org/10.1002/PIP.1156>.
- Becquerel, M.E., 1839. Mémoire sur les effets électriques produits sous l'influence des rayons solaires. C. R. Hebd. Séances Acad. Sci. vol. 9, 561–567.
- Fonash, Stephen J., 2010. Solar Cell Device Physics. Elsevier, <https://doi.org/10.1016/C2009-0-19749-0>.
- Parnis, J.M., Oldham, K.B., 2013. Beyond the beer-lambert law: the dependence of absorbance on time in photochemistry (Sep.). J. Photochem. Photobiol. A Chem. vol. 267, 6–10. <https://doi.org/10.1016/J.JPHOTOCHEM.2013.06.006>.
- (Nov.) Aroutounian,V.2001, Quantum dot solar cells, vol. 445813384510.1117/12.448264(<https://doi.org/10.1117/12.448264>)(Nov.).
- Rehman, Fatima, et al., 2023. Fourth-generation solar cells: a review. Energy Adv. <https://doi.org/10.1039/D3YA00179B>.
- Mohamed, S.A., Abd El Sattar, M., 2019. “A comparative study of P&O and INC maximum power point tracking techniques for grid-connected PV systems,” (Feb.). SN Appl. Sci. vol. 1 (2), 1–13. <https://doi.org/10.1007/S42452-018-0134-4/FIGURES/15>.
- Kirchartz, T., Rau, U., 2018. What makes a good solar cell? (Oct.). Adv. Energy Mater. vol. 8 (28), 1703385. <https://doi.org/10.1002/AENM.201703385>.
- Fritts, C.E., Fritts, C.E., 1883. On a new form of selenium cell, and some electrical discoveries made by its use (Dec.). AmJS vol. 26 (156), 465–472. <https://doi.org/10.2475/AJS.S3-26.156.465>.
- Czochralski, J., 1918. Ein neues Verfahren zur Messung der Kristallisationsgeschwindigkeit der Metalle (Nov.). Z. F. üR. Phys. Chem. vol. 92U (1), 219–221. <https://doi.org/10.1515/ZPCH-1918-9212>.
- Chapin, D.M., Fuller, C.S., Pearson, G.L., Chapin, D.M., Fuller, C.S., Pearson, G.L., 1954. A new silicon p-n junction photocell for converting solar radiation into electrical power. JAP vol. 25 (5), 676–677. <https://doi.org/10.1063/1.1721711>.
- S. Loff, “Vanguard Satellite, 1958,” 2015, Accessed: Jul. 30, 2023. [Online]. Available: <http://www.nasa.gov/content/vanguard-satellite-1958>.
- Yamaguchi, M., Dimroth, F., Geisz, J.F., Elkins-Daukes, N.J., 2021. Multi-junction solar cells paving the way for super high-efficiency,” (Jun.). J. Appl. Phys. vol. 129 (24), 240901. <https://doi.org/10.1063/5.0048653/523212>.
- Arunmetha, S., et al., 2017. Study on production of silicon nanoparticles from quartz sand for hybrid solar cell applications (Sep.). J. Electron. Mater. vol. 47 (1), 493–502. <https://doi.org/10.1007/S11664-017-5794-0>.

- Ferrazza, F., 2012. Crystalline Silicon: Manufacture and Properties (Jan.). Pract. Handb. Photovolt. 79–97. <https://doi.org/10.1016/B978-0-12-385934-1.00004-0>.
- Wilson, G.M., et al., 2020. The 2020 photovoltaic technologies roadmap (Sep.). J. Phys. D. Appl. Phys. vol. 53 (49), 493001. <https://doi.org/10.1088/1361-6463/AB9C6A>.
- S. Philipps, F. Ise, W. Warmuth, and P. Projects GmbH, "Photovoltaics Report", Accessed: Aug. 08, 2023. [Online]. Available: [www.ise.fraunhofer.de](http://www.ise.fraunhofer.de).
- Anon, "Commercial Solar Panel Efficiency: What You Need to Know." Accessed: Sep. 14, 2023b. [Online]. Available: <https://www.velosolar.com/solar-panel-efficiency/>.
- Green, M.A., 1993. Silicon solar cells: evolution, high-efficiency design and efficiency enhancements (Jan.). Semicond. Sci. Technol. vol. 8 (1), 1. <https://doi.org/10.1088/0268-1242/8/1/001>.
- Mandelkorn, J., McAfee, C., Kesperis, J., Schwartz, L., Pharo, W., 1962. Fabrication and Characteristics of Phosphorous-Diffused Silicon Solar Cells (Apr.). J. Electrochem. Soc. vol. 109 (4), 313. <https://doi.org/10.1149/1.2425407>.
- Mandelkorn, J., Lamneck, J.H., 1973. A new electric field effect in silicon solar cells (Oct.). J. Appl. Phys. vol. 44 (10), 4785–4787. <https://doi.org/10.1063/1.1662040>.
- Lindmayer, J., Allison, J.F., 1990. "Violet cell": an improved silicon solar cell. COMSAT Tech. Rev. ; (U.S.) vol. 3:1 (2–3), 151–166. [https://doi.org/10.1016/0379-6787\(90\)90023-X](https://doi.org/10.1016/0379-6787(90)90023-X).
- Green, M.A., Blakers, A.W., Narayanan, S., Taouk, M., 1986. Improvements in silicon solar cell efficiency (Mar.). Sol. Cells vol. 17 (1), 75–83. [https://doi.org/10.1016/0379-6787\(86\)90060-8](https://doi.org/10.1016/0379-6787(86)90060-8).
- Ribeiro, P.J., 2017. Crystalline silicon solar cells: Better than ever (May). Nat. Energy vol. 2 (5), 1–2. <https://doi.org/10.1038/nenergy.2017.67>.
- Yoshikawa, K., et al., 2017. Silicon heterojunction solar cell with interdigitated back contacts for a photoconversion efficiency over 26% (Mar.). Nat. Energy vol. 2 (5), 1–8. <https://doi.org/10.1038/nenergy.2017.32>.
- Qarony, W., et al., 2017. Efficient amorphous silicon solar cells: characterization, optimization, and optical loss analysis (Jan.). Results Phys. vol. 7, 4287–4293. <https://doi.org/10.1016/J.RINP.2017.09.030>.
- Iddha, A., Ayat, L., Dahbi, N., 2023. Improving the performance of hydrogenated amorphous silicon solar cell using a-si:Ge:H alloy. J. Ovonics Res. vol. 15 (5), 271–278.
- Yu, Z., et al., 2019a. Improved power conversion efficiency in radial junction thin film solar cells based on amorphous silicon germanium alloys (Sep.). J. Alloy. Compd. vol. 803, 260–264. <https://doi.org/10.1016/J.JALLCOM.2019.06.276>.
- Hsu, C.H., Zhang, X.Y., Zhao, M.J., Lin, H.J., Zhu, W.Z., Lien, S.Y., 2019. Silicon Heterojunction solar cells with p-type silicon carbon window layer (Aug.). Crystals vol. 9 (8), 402. <https://doi.org/10.3390/CRYST9080402>.
- Ramanujam, J., et al., 2020. Flexible CIGS, CdTe and a-Si:H based thin film solar cells: a review (May). Prog. Mater. Sci. vol. 110, 100619. <https://doi.org/10.1016/J.PMATSCL.2019.100619>.
- Moutinho, H.R., Hasoon, F.S., Abulfotuh, F., Kazmerski, L.L., 1995. Investigation of polycrystalline CdTe thin films deposited by physical vapor deposition, close-spaced sublimation, and sputtering (Nov.). J. Vac. Sci. Technol. A vol. 13 (6), 2877–2883. <https://doi.org/10.1116/1.579607>.
- Kartopu, G., et al., 2016. Progression of metalorganic chemical vapour-deposited CdTe thin-film PV devices towards modules (Mar.). Prog. Photovolt.: Res. Appl. vol. 24 (3), 283–291. <https://doi.org/10.1002/PIP.2668>.
- Anon "Cadmium Telluride | Department of Energy." Accessed: Aug. 04, 2023c. [Online]. Available: <https://www.energy.gov/eere/solar/cadmium-telluride>.
- Anon, "Copper Indium Gallium Diselenide | Department of Energy." Accessed: Aug. 04, 2023d. [Online]. Available: <https://www.energy.gov/eere/solar/copper-indium-gallium-diselenide>.
- Efazli, E.T., et al., 2021. A review of primary technologies of thin-film solar cells (Sep.). Eng. Res. Express vol. 3 (3), 032001. <https://doi.org/10.1088/2631-8695/AC2353>.
- Adamovic, N., Zimmermann, A., Caviasca, A., Harboe, R., Ibanez, F., 2017. "Custom designed photovoltaic modules for PIPV and BIPV applications," (Mar.). J. Renew. Sustain. Energy vol. 9 (2). <https://doi.org/10.1063/1.4979820/153122>.
- Moon, Md.M.A., Rahman, Md.F., Hossain, J., Ismail, A.B. Md, 2019. Comparative study of the second generation a-Si:H, CdTe, and CIGS thin-film solar cells (Jun.). Adv. Mat. Res vol. 1154, 102–111. <https://doi.org/10.4028/WWW.SCIENTIFIC.NET/AMR.1154.102>.
- Green, M.A., 2002. Third generation photovoltaics: solar cells for 2020 and beyond (Apr.). Phys. E Low. Dimens. Syst. Nanostruct. vol. 14 (1–2), 65–70. [https://doi.org/10.1016/S1386-9477\(02\)00361-2](https://doi.org/10.1016/S1386-9477(02)00361-2).
- Chopra, K.L., Paulson, P.D., Dutta, V., 2004. Thin-film solar cells: an overview (Mar.). Prog. Photovolt.: Res. Appl. vol. 12 (2–3), 69–92. <https://doi.org/10.1002/PIP.541>.
- Kojima, A., Teshima, K., Shirai, Y., Miyasaka, T., 2009. "Organometal halide perovskites as visible-light sensitizers for photovoltaic cells," (May). J. Am. Chem. Soc. vol. 131 (17), 6050–6051. [https://doi.org/10.1021/JA809598R/SUPPLFILE/JA809598R\\_SI\\_001.PDF](https://doi.org/10.1021/JA809598R/SUPPLFILE/JA809598R_SI_001.PDF).
- Anon "Perovskite Solar Cells | Department of Energy." Accessed: Aug. 05, 2023e. [Online]. Available: <https://www.energy.gov/eere/solar/perovskite-solar-cells>.
- Green, M.A., Ho-Baillie, A., Snaith, H.J., 2014. The emergence of perovskite solar cells (Jun.). Nat. Photonics vol. 8 (7), 506–514. <https://doi.org/10.1038/nphoton.2014.134>.
- Li, H., et al., 2022. "Sequential vacuum-evaporated perovskite solar cells with more than 24% efficiency," (Jul.). Sci. Adv. vol. 8 (28), 7422. [https://doi.org/10.1126/SCIAADV.ABO7422/SUPPLFILE/SCIAADV.ABO7422\\_MOVIES\\_S1\\_AND\\_S2.ZIP.ZIP](https://doi.org/10.1126/SCIAADV.ABO7422/SUPPLFILE/SCIAADV.ABO7422_MOVIES_S1_AND_S2.ZIP.ZIP).
- Hoppe, H., Sariciftci, N.S., 2004. Organic solar cells: an overview (Jul.). J. Mater. Res vol. 19 (7), 1924–1945. <https://doi.org/10.1557/JMR.2004.0252>.
- Yin, Z., Wei, J., Zheng, Q., 2016. Interfacial materials for organic solar cells: recent advances and perspectives (Aug.). Adv. Sci. vol. 3 (8), 1500362. <https://doi.org/10.1002/ADVS.201500362>.
- Benanti, T.L., Venkataraman, D., 2006. "Organic solar cells: An overview focusing on active layer morphology," (Jan.). Photosynth Res vol. 87 (1), 73–81. <https://doi.org/10.1007/S11120-005-6397-9/METRICS>.
- Lu, L., Zheng, T., Wu, Q., Schneider, A.M., Zhao, D., Yu, L., 2015. "Recent advances in bulk heterojunction polymer solar cells," (Dec.). Chem. Rev. vol. 115 (23), 12666–12731. [https://doi.org/10.1021/ACS.CHEMREV.5B00098/ASSET/IMAGES/ACS.CHEMREV.5B00098.SOICAL.JPEG\\_V03](https://doi.org/10.1021/ACS.CHEMREV.5B00098/ASSET/IMAGES/ACS.CHEMREV.5B00098.SOICAL.JPEG_V03).
- Cui, Y., et al., 2019. Over 16% efficiency organic photovoltaic cells enabled by a chlorinated acceptor with increased open-circuit voltages (Jun.). Nat. Commun. vol. 10 (1), 1–8. <https://doi.org/10.1038/s41467-019-10351-5>.
- Meng, L., et al., 2018. Organic and solution-processed tandem solar cells with 17.3% efficiency (Sep.). Science (1979) vol. 361 (6407), 1094–1098. [https://doi.org/10.1126/SCIENCE.AAT2612/SUPPLFILE/AAT2612\\_MENG\\_SM.PDF](https://doi.org/10.1126/SCIENCE.AAT2612/SUPPLFILE/AAT2612_MENG_SM.PDF).
- Anon, "Interactive Best Research-Cell Efficiency Chart | Photovoltaic Research | NREL." Accessed: Aug. 04, 2023f. [Online]. Available: <https://www.nrel.gov/pv/interactive-cell-efficiency.html>.
- Chao, Y.C., et al., 2023. Unconventional organic solar cell structure based on hyperbolic metamaterial (Feb.). J. Mater. Chem. C. Mater. vol. 11 (6), 2273–2281. <https://doi.org/10.1039/D2TC04723C>.
- Grätzel, M., 2003. Dye-sensitized solar cells (Oct.). J. Photochem. Photobiol. C: Photocem. Rev. vol. 4 (2), 145–153. [https://doi.org/10.1016/S1389-5567\(03\)00026-1](https://doi.org/10.1016/S1389-5567(03)00026-1).
- Bose, S., Soni, V., Genwa, K.R., 2015. Recent Advances and Future Prospects for Dye Sensitized Solar Cells: A Review. Int. J. Sci. Res. Publ. vol. 5 (4). Accessed: Aug. 19, 2023. [Online]. Available: [www.ijrsp.org](http://www.ijrsp.org).
- Çakar, S., Özçar, M., Findik, F., 2022. MOFs-based dye-sensitized photovoltaics (Jan.). Met.-Org. Framew.-Based Nanomater. Energy Convers. Storage 487–506. <https://doi.org/10.1016/B978-0-323-91179-5.00033-4>.
- Kunzmann, A., et al., 2018. Hybrid dye-titania nanoparticles for superior low-temperature dye-sensitized solar cells (Apr.). Adv. Energy Mater. vol. 8 (12). <https://doi.org/10.1002/AENM.201702583>.
- Kakiage, K., Aoyama, Y., Yano, T., Oya, K., Fujisawa, J.I., Hanaya, M., 2015. Highly-efficient dye-sensitized solar cells with collaborative sensitization by silyl-anchor and carboxy-anchor dyes (Oct.). Chem. Commun. vol. 51 (88), 15894–15897. <https://doi.org/10.1039/C5CC06759F>.
- Ren, Y., et al., 2022. Hydroxamic acid pre-adsorption raises the efficiency of cosensitized solar cells. Nature vol. 613 (7942), 60–65. <https://doi.org/10.1038/s41586-022-05460-z>.
- Zhou, Y., Herz, L.M., Jen, A.K.Y., Saliba, M., 2022. Advances and challenges in understanding the microscopic structure–property–performance relationship in perovskite solar cells (Sep.). Nat. Energy vol. 7 (9), 794–807. <https://doi.org/10.1038/s41560-022-01096-5>.
- Geim, A.K., Novoselov, K.S., 2007. The rise of graphene (Mar.). Nat. Mater. vol. 6 (3), 183–191. <https://doi.org/10.1038/nmat1849>.
- Bonaccorso, F., Sun, Z., Hasan, T., Ferrari, A.C., 2010. Graphene photonics and optoelectronics (Sep.). Nat. Photonics vol. 4 (9), 611–622. <https://doi.org/10.1038/NPHOTON.2010.186>.
- Park, H., Brown, P.R., Bulović, V., Kong, J., 2012. "Graphene as transparent conducting electrodes in organic photovoltaics: Studies in graphene morphology, hole transporting layers, and counter electrodes," (Jan.). Nano Lett. vol. 12 (1), 133–140. [https://doi.org/10.1021/NL2029859/SUPPLFILE/NL2029859\\_SI\\_001.PDF](https://doi.org/10.1021/NL2029859/SUPPLFILE/NL2029859_SI_001.PDF).
- Wang, X., Zhi, L., Müllen, K., 2008. "Transparent, conductive graphene electrodes for dye-sensitized solar cells," (Jan.). Nano Lett. vol. 8 (1), 323–327. [https://doi.org/10.1021/NL072838RNL072838RSI20071031\\_120726.PDF](https://doi.org/10.1021/NL072838RNL072838RSI20071031_120726.PDF).
- Zhang, C., et al., 2019. Efficient stable graphene-based perovskite solar cells with high flexibility in device assembling via modular architecture design (Dec.). Energy Environ. Sci. vol. 12 (12), 3585–3594. <https://doi.org/10.1039/C9EE02391G>.
- Kumar, R., Sharma, A.K., Bhatnagar, M., Mehta, B.R., Rath, S., 2013. Antireflection properties of graphene layers on planar and textured silicon surfaces (Mar.). Nanotechnology vol. 24 (16), 165402. <https://doi.org/10.1088/0957-4484/24/16/165402>.
- Liu, J., et al., 2012a. Hole and electron extraction layers based on graphene oxide derivatives for high-performance bulk heterojunction solar cells (May). Adv. Mater. vol. 24 (17), 2228–2233. <https://doi.org/10.1002/ADMA.201104945>.
- Liu, J., Xue, Y., Zhang, M., Dai, L., 2012b. Graphene-based materials for energy applications (Nov.). MRS Bull. vol. 37 (12), 1265–1272. <https://doi.org/10.1557/MRS.2012.179>.
- Iqbal, M.A., et al., 2022. Materials for Photovoltaics: Overview, Generations, Recent Advancements and Future Prospects (Jan.). Thin Films Photovolt.. <https://doi.org/10.5772/INTECHOPEN.101449>.
- Loh, K.P., Tong, S.W., Wu, J., 2016. "Graphene and Graphene-like Molecules: Prospects in Solar Cells," (Feb.). J. Am. Chem. Soc. vol. 138 (4), 1095–1102. [https://doi.org/10.1021/JACS.5B10917/ASSET/IMAGES/MEDIUM/JA-2015-10917C\\_0005.GIF](https://doi.org/10.1021/JACS.5B10917/ASSET/IMAGES/MEDIUM/JA-2015-10917C_0005.GIF).
- Chen, Y., Lin, W.C., Liu, J., Dai, L., 2014. "Graphene oxide-based carbon interconnecting layer for polymer tandem solar cells," (Mar.). Nano Lett. vol. 14 (3), 1467–1471. [https://doi.org/10.1021/NL4046284/SUPPLFILE/NL4046284\\_SI\\_002.PDF](https://doi.org/10.1021/NL4046284/SUPPLFILE/NL4046284_SI_002.PDF).
- Wang, Y., Sun, T., Paudel, T., Zhang, Y., Ren, Z., Kempa, K., 2012. "Metamaterial-plasmonic absorber structure for high efficiency amorphous silicon solar cells," (Jan.). Nano Lett. vol. 12 (1), 440–445. [https://doi.org/10.1021/NL203763K/ASSET/IMAGES/MEDIUM/NL-2011-03763K\\_0001.GIF](https://doi.org/10.1021/NL203763K/ASSET/IMAGES/MEDIUM/NL-2011-03763K_0001.GIF).
- Abdulkarim, Y.I., et al., 2022. "A Review on Metamaterial Absorbers: Microwave to Optical," (Apr.). Front. Phys. vol. 10, 893791. <https://doi.org/10.3389/FPHY.2022.893791/BIBTEX>.
- Hossain, M.J., Rahman, Md.H., Faruque, M.R.I., 2023. An Innovative Polarisation-Insensitive Perfect Metamaterial Absorber with an Octagonal-Shaped Resonator for

- Energy Harvesting at Visible Spectra (Jun.). *Nanomaterials* vol. 13 (12), 1882. <https://doi.org/10.3390/NANO13121882>.
- Karami, S., Nikoufard, M., Sharatiadmar, S.M., Javadi, S., 2021. Plasmonic hyperbolic metamaterial and nanosphere composite for light trapping as a solar cell: Numerical study (Dec.). *Opt. Mater. (Amst.)* vol. 122, 111740. <https://doi.org/10.1016/J.OPMATERIALS.2021.111740>.
- Hamouche, H., Shabat, M.M., Schaadt, D.M., 2017. Multilayer solar cell waveguide structures containing metamaterials (Jan.). *Superlattices Micro* vol. 101, 633–640. <https://doi.org/10.1016/J.SPMI.2016.08.047>.
- Jing, H., et al., 2020. “Hybrid organic-inorganic perovskite metamaterial for light trapping and photon-to-electron conversion,” (Sep.). *Nanophotonics* vol. 9 (10), 3323–3333. [https://doi.org/10.1515/NANOPH-2020-0071/ASSET/GRAPHIC/J\\_NANOPH-2020-0071 FIG\\_007.JPG](https://doi.org/10.1515/NANOPH-2020-0071/ASSET/GRAPHIC/J_NANOPH-2020-0071 FIG_007.JPG).
- Bossard, J.A., Lin, L., Yun, S., Liu, L., Werner, D.H., Mayer, T.S., 2014. “Near-ideal optical metamaterial absorbers with super-octave bandwidth,” (Feb.). *ACS Nano* vol. 8 (2), 1517–1524. [https://doi.org/10.1021/NN4057148/SUPPL\\_FILE/NN4057148\\_SI\\_001.PDF](https://doi.org/10.1021/NN4057148/SUPPL_FILE/NN4057148_SI_001.PDF).
- Yu, P., et al., 2019b. Broadband Metamaterial Absorbers (Feb.). *Adv. Opt. Mater.* vol. 7 (3), 1800995. <https://doi.org/10.1002/ADOM.201800995>.
- Fraas, L.M., Avery, J.E., Huang, H.X., Harder, N.-P., Urfei, P.W., 2003. Theoretical limits of thermophotovoltaic solar energy conversion (Apr.). *Semicond. Sci. Technol.* vol. 18 (5), S151. <https://doi.org/10.1088/0268-1242/18/5/303>.
- Dincer, F., Akgol, O., Karaaslan, M., Unal, E., Sabah, C., 2014. Polarization angle independent perfect metamaterial absorbers for solar cell applications in the microwave, infrared, and visible regime. *Prog. Electromagn. Res.* vol. 144, 93–101. <https://doi.org/10.2528/PIER13111404>.
- Li, W., et al., 2014. Refractory plasmonics with titanium nitride: broadband metamaterial absorber (Dec.). *Adv. Mater.* vol. 26 (47), 7959–7965. <https://doi.org/10.1002/ADMA.201401874>.
- Günay, D., Koschny, T., Soukoulis, C.M., 2009. “Reducing ohmic losses in metamaterials by geometric tailoring,” (Sep.). *Phys. Rev. B Condens Matter Mater. Phys.* vol. 80 (12), 125129. <https://doi.org/10.1103/PHYSREVB.80.125129/FIGURES/7/MEDIUM>.
- Green, M.A., 2015. The Passivated Emitter and Rear Cell (PERC): From conception to mass production (Dec.). *Sol. Energy Mater. Sol. Cells* vol. 143, 190–197. <https://doi.org/10.1016/J.SOLMAT.2015.06.055>.
- Matsui, T., et al., 2015. High-efficiency amorphous silicon solar cells: Impact of deposition rate on metastability (Feb.). *Appl. Phys. Lett.* vol. 106 (5). <https://doi.org/10.1063/1.4907001>.
- Sai, H., Matsui, T., Kumagai, H., Matsubara, K., 2018. “Thin-film microcrystalline silicon solar cells: 11.9% efficiency and beyond,” (Feb.). *Appl. Phys. Express* vol. 11 (2), 022301. <https://doi.org/10.7567/APEX.11.022301/XML>.
- Green, M.A., et al., 2023. Solar cell efficiency tables (version 62) (Jul.). *Prog. Photovolt. Res. Appl.* vol. 31 (7), 651–663. <https://doi.org/10.1002/PIP.3726>.
- Anon, “Systems and methods for advanced ultra-high-performance InP solar cells,” Mar. 2014.
- Zhu, L., et al., 2022. Single-junction organic solar cells with over 19% efficiency enabled by a refined double-fibril network morphology (Jun.). *Nat. Mater.* vol. 21 (6), 656–663. <https://doi.org/10.1038/S41563-022-01244-Y>.
- Ren, Y., et al., 2023. Hydroxamic acid pre-adsorption raises the efficiency of co-sensitized solar cells (Jan.). *Nature* vol. 613 (7942), 60–65. <https://doi.org/10.1038/S41586-022-05460-Z>.
- Geisz, J.F., et al., 2018. Building a six-junction inverted metamorphic concentrator solar cell (Mar.). *IEEE J. Photo* vol. 8 (2), 626–632. <https://doi.org/10.1109/JPHOTOV.2017.2778567>.
- Lin, R., et al., 2022. All-perovskite tandem solar cells with improved grain surface passivation (Jan.). *Nature* vol. 603 (7899), 73–78. <https://doi.org/10.1038/S41586-021-04372-8>.
- Chen, W., et al., 2022. Monolithic perovskite/organic tandem solar cells with 23.6% efficiency enabled by reduced voltage losses and optimized interconnecting layer (Mar.). *Nat. Energy* vol. 7 (3), 229–237. <https://doi.org/10.1038/S41560-021-00966-8>.
- Shockley, W., Queisser, H.J., 1961. Detailed balance limit of efficiency of p-n junction solar cells. *J. Appl. Phys.* vol. 32 (3), 510–519. <https://doi.org/10.1063/1.1736034>.
- Kumar, A., Kumar, Ankush, 2017. Predicting efficiency of solar cells based on transparent conducting electrodes (Jan.). *JAP* vol. 121 (1), 014502. <https://doi.org/10.1063/1.4973117>.
- Kim, N., Kim, D., Kang, H., Park, Y.G., 2016. Improved heat dissipation in a crystalline silicon PV module for better performance by using a highly thermal conducting backsheet (Oct.). *Energy* vol. 113, 515–520. <https://doi.org/10.1016/J.ENERGY.2016.07.046>.
- Wang, A., Xuan, Y., 2018. A detailed study on loss processes in solar cells (Feb.). *Energy* vol. 144, 490–500. <https://doi.org/10.1016/J.ENERGY.2017.12.058>.
- Hirst, L.C., Ekins-Daukes, N.J., 2011. Fundamental losses in solar cells (May). *Prog. Photovolt.: Res. Appl.* vol. 19 (3), 286–293. <https://doi.org/10.1002/PIP.1024>.
- Dupré, O., Vaillon, R., Green, M.A., 2016. A full thermal model for photovoltaic devices (Dec.). *Sol. Energy* vol. 140, 73–82. <https://doi.org/10.1016/J.SOLENER.2016.10.033>.
- C.M. Garner, and Garner C.M., “Extrinsic losses in solar cells for linear focus systems 4,” STIN, vol. 80, p. 24842, 1979, Accessed: Aug. 12, 2023. [Online]. Available: (<https://ui.adsabs.harvard.edu/abs/1979STIN.8024842G/abstract>).
- Abdullah, M.F., et al., 2016. Research and development efforts on texturization to reduce the optical losses at front surface of silicon solar cell (Dec.). *Renew. Sustain. Energy Rev.* vol. 66, 380–398. <https://doi.org/10.1016/J.RSER.2016.07.065>.
- Wang, H.-P., He, J.-H., Wang, H.-P., He, J.-H., 2017. Toward Highly Efficient Nanostructured Solar Cells Using Concurrent Electrical and Optical Design (Dec.). *Adv. Energy Mater.* vol. 7 (23), 1602385. <https://doi.org/10.1002/AENM.201602385>.
- Fell, A., et al., 2022. Modeling parasitic absorption in silicon solar cells with a near-surface absorption parameter (Mar.). *Sol. Energy Mater. Sol. Cells* vol. 236, 111534. <https://doi.org/10.1016/J.SOLMAT.2021.111534>.
- Werner, J., et al., 2016a. “Parasitic Absorption Reduction in Metal Oxide-Based Transparent Electrodes: Application in Perovskite Solar Cells,” (Jul.). *ACS Appl. Mater. Interfaces* vol. 8 (27), 17260–17267. [https://doi.org/10.1021/ACSAMI.6B04425/SUPPL\\_FILE/AM6B04425\\_SI\\_001.PDF](https://doi.org/10.1021/ACSAMI.6B04425/SUPPL_FILE/AM6B04425_SI_001.PDF).
- Pysch, D., Mette, A., Glunz, S.W., 2007. A review and comparison of different methods to determine the series resistance of solar cells (Nov.). *Sol. Energy Mater. Sol. Cells* vol. 91 (18), 1698–1706. <https://doi.org/10.1016/J.SOLMAT.2007.05.026>.
- Servaites, J.D., Yeganeh, S., Marks, T.J., Ratner, M.A., 2010. Efficiency enhancement in organic photovoltaic cells: consequences of optimizing series resistance (Jan.). *Adv. Funct. Mater.* vol. 20 (1), 97–104. <https://doi.org/10.1002/ADM.200901107>.
- Gupta, D.K., Langelaar, M., Barink, M., van Keulen, F., 2015. Topology optimization of front metallization patterns for solar cells (Apr.). *Struct. Multidiscip. Optim.* vol. 51 (4), 941–955. <https://doi.org/10.1007/S00158-014-1185-9>.
- Fathi, M., Abderrezek, M., Friedrich, M., 2017. “Reducing dust effects on photovoltaic panels by hydrophobic coating,” (Mar.). *Clean. Technol. Environ. Policy* vol. 19 (2), 577–585. <https://doi.org/10.1007/S10098-016-1233-9/FIGURES/12>.
- Sarkin, A.S., Ekren, N., Sağlam, Ş., 2020. A review of anti-reflection and self-cleaning coatings on photovoltaic panels (Mar.). *Sol. Energy* vol. 199, 63–73. <https://doi.org/10.1016/J.SOLENER.2020.01.084>.
- Jošt, M., et al., 2017. “Efficient light management by textured nanoimprinted layers for perovskite solar cells,” (May). *ACS Photonics* vol. 4 (5), 1232–1239. [https://doi.org/10.1021/ACSPHOTONICS.7B00138/SUPPL\\_FILE/PH7B00138\\_SI\\_001.PDF](https://doi.org/10.1021/ACSPHOTONICS.7B00138/SUPPL_FILE/PH7B00138_SI_001.PDF).
- Hsiao, Y.S., et al., 2012. “Improving the light trapping efficiency of plasmonic polymer solar cells through photon management,” (Oct.). *J. Phys. Chem. C* vol. 116 (39), 20731–20737. [https://doi.org/10.1021/JP306124N/SUPPL\\_FILE/JP306124N\\_SI\\_001.PDF](https://doi.org/10.1021/JP306124N/SUPPL_FILE/JP306124N_SI_001.PDF).
- Curtin, B., Biswas, R., Dalal, V., 2009. “Photonic crystal based back reflectors for light management and enhanced absorption in amorphous silicon solar cells,” (Dec.). *Appl. Phys. Lett.* vol. 95 (23). <https://doi.org/10.1063/1.3269593/120883>.
- Addie, A.J., Ismail, R.A., Mohammed, M.A., 2022. Amorphous carbon nitride dual-function anti-reflection coating for crystalline silicon solar cells (Jun.). *Sci. Rep.* vol. 12 (1), 1–12. <https://doi.org/10.1038/s41598-022-14078-0>.
- Forberich, K., Dennler, G., Schärber, M.C., Hingerl, K., Fromherz, T., Brabec, C.J., 2008. Performance improvement of organic solar cells with moth eye anti-reflection coating (Aug.). *Thin Solid Films* vol. 516 (20), 7167–7170. <https://doi.org/10.1016/J.TSF.2007.12.088>.
- Sahouane, N., Zerga, A., 2014. Optimization of antireflection multilayer for industrial crystalline silicon solar cells (Jan.). *Energy Procedia* vol. 44, 118–125. <https://doi.org/10.1016/J.EGYPRO.2013.12.017>.
- Papet, P., et al., 2006. Pyramidal texturing of silicon solar cell with TMAH chemical anisotropic etching (Sep.). *Sol. Energy Mater. Sol. Cells* vol. 90 (15), 2319–2328. <https://doi.org/10.1016/J.SOLMAT.2006.03.005>.
- Cho, C., et al., 2013. Random and V-groove texturing for efficient light trapping in organic photovoltaic cells (Aug.). *Sol. Energy Mater. Sol. Cells* vol. 115, 36–41. <https://doi.org/10.1016/J.SOLMAT.2013.03.014>.
- Li, P., Xie, J., Cheng, J., Jiang, Y.N., 2015. Study on weak-light photovoltaic characteristics of solar cell with a microgroove lens array on glass substrate (Apr.). *Opt. Express* vol. 23 (7), A192. <https://doi.org/10.1364/OE.23.00A192>.
- Moulin, E., Paetzold, U., Wilhelm, Siekmann, H., Werbs, J., Bauer, A., Carius, R., 2011. Study of thin-film silicon solar cell back reflectors and potential of detached reflectors (Jan.). *Energy Procedia* vol. 10, 106–110. <https://doi.org/10.1016/J.EGYPRO.2011.10.161>.
- Kim, M.S., Lee, J.H., Kwak, M.K., 2020. “Review: Surface Texturing Methods for Solar Cell Efficiency Enhancement,” (Jul.). *Int. J. Precis. Eng. Manuf.* vol. 21 (7), 1389–1398. <https://doi.org/10.1007/S12541-020-00337-5/FIGURES/10>.
- de Aberasturi, D.J., Serrano-Montes, A.B., Liz-Marzán, L.M., 2015. “Modern Applications of Plasmonic Nanoparticles: From Energy to Health (May). *Adv. Opt. Mater.* vol. 3 (5), 602–617. <https://doi.org/10.1002/ADOM.201500053>.
- Erwin, W.R., Zarick, H.F., Talbert, E.M., Bardhan, R., 2016. Light trapping in mesoporous solar cells with plasmonic nanostructures (May). *Energy Environ. Sci.* vol. 9 (5), 1577–1601. <https://doi.org/10.1039/C5EE03847B>.
- Matheu, P., Lim, S.H., Derkacs, D., McPheeers, C., Yu, E.T., 2008. “Metal and dielectric nanoparticle scattering for improved optical absorption in photovoltaic devices,” (Sep.). *Appl. Phys. Lett.* vol. 93 (11). <https://doi.org/10.1063/1.2957980/335396>.
- Pfeiffer, T.V., et al., 2014. Plasmonic Nanoparticle Films for Solar Cell Applications Fabricated by Size-selective Aerosol Deposition (Jan.). *Energy Procedia* vol. 60 (C), 3–12. <https://doi.org/10.1016/J.EGYPRO.2014.12.335>.
- Prabhathan, P., Murukeshan, V.M., 2016. “Surface Plasmon Polariton-coupled Waveguide Back Reflector in Thin-film Silicon Solar Cell,” (Feb.). *Plasmonics* vol. 11 (1), 253–260. <https://doi.org/10.1007/S11468-015-0045-9/TABLES/1>.
- Beck, F.J., Polman, A., Catchpole, K.R., 2009. “Tunable light trapping for solar cells using localized surface plasmons,” (Jun.). *J. Appl. Phys.* vol. 105 (11). <https://doi.org/10.1063/1.3140609/146499>.
- H.A. Atwater and A. Polman, “Plasmonics for improved photovoltaic devices,” *Nature Materials* 2010 9:3 , vol. 9, no. 3, pp. 205–213, Feb. 2010, doi: 10.1038/nmat2629.
- Zambree, A.S., Bermakai, M.Y., Yusoff, M.Z.M., 2023. Modelling and optimization of a light trapping scheme in a silicon solar cell using silicon nitride (sinx) anti-reflective coating (May). *Trends Sci.* vol. 20 (9), 5555. <https://doi.org/10.48048/tis.2023.5555>.

- Stan, M., et al., 2008. Very high efficiency triple junction solar cells grown by MOVPE (Nov.). *J. Cryst. Growth* vol. 310 (23), 5204–5208. <https://doi.org/10.1016/J.JCRYSGRO.2008.07.024>.
- Philipps, S.P., Dimroth, F., Bett, A.W., 2018. High-Efficiency III-V multijunction solar cells (Jan.). *McEvoy'S. Handb. Photovolt.: Fundam. Appl.* 439–472. <https://doi.org/10.1016/B978-0-12-809921-6.00012-4>.
- McKenna, B., Evans, R.C., 2017. Towards efficient spectral converters through materials design for luminescent solar devices (Jul.). *Adv. Mater.* vol. 29 (28), 1606491. <https://doi.org/10.1002/ADMA.201606491>.
- Van Der Ende, B.M., Aarts, L., Meijerink, A., 2009. Lanthanide ions as spectral converters for solar cells (Nov.). *Phys. Chem. Chem. Phys.* vol. 11 (47), 11081–11095. <https://doi.org/10.1039/B913877C>.
- Huang, X., Han, S., Huang, W., Liu, X., 2012. Enhancing solar cell efficiency: the search for luminescent materials as spectral converters (Dec.). *Chem. Soc. Rev.* vol. 42 (1), 173–201. <https://doi.org/10.1039/C2CS35288E>.
- Zhang, Q.Y., Huang, X.Y., 2010. Recent progress in quantum cutting phosphors (Jul.). *Prog. Mater. Sci.* vol. 55 (5), 353–427. <https://doi.org/10.1016/J.PMATSCL.2009.10.001>.
- Wang, F., Banerjee, D., Liu, Y., Chen, X., Liu, X., 2010. Upconversion nanoparticles in biological labeling, imaging, and therapy (Aug.). *Analyst* vol. 135 (8), 1839–1854. <https://doi.org/10.1039/COAN00144A>.
- Ramiro, I., Martí, A., 2021. Intermediate band solar cells: Present and future (Jul.). *Prog. Photovolt.: Res. Appl.* vol. 29 (7), 705–713. <https://doi.org/10.1002/PIP.3351>.
- Luque, A., Martí, A., Stanley, C., 2012. Understanding intermediate-band solar cells (Feb.). *Nat. Photonics* vol. 6 (3), 146–152. <https://doi.org/10.1038/nphoton.2012.1>.
- Popescu, V., Bester, G., Hanna, M.C., Norman, A.G., Zunger, A., 2008. “Theoretical and experimental examination of the intermediate-band concept for strain-balanced (In, Ga)As/Ga(As,P) quantum dot solar cells,” (Nov.). *Phys. Rev. B Condens Matter Mater. Phys.* vol. 78 (20), 205321. <https://doi.org/10.1103/PHYSREVB.78.205321/FIGURES/16/MEDIUM>.
- Luque, A., et al., 2004. General equivalent circuit for intermediate band devices: Potentials, currents and electroluminescence (Jul.). *J. Appl. Phys.* vol. 96 (1), 903–909. <https://doi.org/10.1063/1.1760836>.
- Luque, A., Martí, A., 2001. A metallic intermediate band high efficiency solar cell (Mar.). *Prog. Photovolt.: Res. Appl.* vol. 9 (2), 73–86. <https://doi.org/10.1002/PIP.354>.
- Marsen, B., Klemz, S., Unold, T., Schock, H.W., 2012. Investigation of the Sub-Bandgap Photoresponse in CuGaS<sub>2</sub>: Fe for Intermediate Band Solar Cells (Sep.). *Prog. Photovolt.: Res. Appl.* vol. 20 (6), 625–629. <https://doi.org/10.1002/PIP.1197>.
- Yu, K.M., et al., 2003. “Diluted ii-vi oxide semiconductors with multiple band gaps,” (Dec.). *Phys. Rev. Lett.* vol. 91 (24), 246403. <https://doi.org/10.1103/PHYSREVLTT.91.246403/FIGURES/4/MEDIUM>.
- Ekins-Daukes, N.J., Schmidt, T.W., 2008. “A molecular approach to the intermediate band solar cell: The symmetric case,” (Aug.). *Appl. Phys. Lett.* vol. 93 (6). <https://doi.org/10.1063/1.2970157/323013>.
- Anon “Home - SolarPower Europe.” Accessed: Aug. 06, 2023g. [Online]. Available: <https://www.solarpowereurope.org/>.
- Smith, D.D., Cousins, P., Westerberg, S., Jesus-Tabajonda, R.De, Aniero, G., Shen, Y.C., 2014. Toward the practical limits of silicon solar cells. *IEEE J. Photo. vol.* 4 (6), 1465–1469. <https://doi.org/10.1109/JPHOTOV.2014.2350695>.
- Shah, A.V., et al., 2004. Thin-film silicon solar cell technology (Mar.). *Prog. Photovolt.: Res. Appl.* vol. 12 (2–3), 113–142. <https://doi.org/10.1002/PIP.533>.
- Akimov, Y.A., Ostrivov, K., Li, E.P., 2009. “Surface plasmon enhancement of optical absorption in thin-film silicon solar cells,” (Jun.). *Plasmonics* vol. 4 (2), 107–113. <https://doi.org/10.1007/S11468-009-9080-8/FIGURES/7>.
- Dubey, R.S., Saravanan, S., Kalainathan, S., 2014. “Performance enhancement of thin film silicon solar cells based on distributed Bragg reflector & diffraction grating,” (Dec.). *AIP Adv.* vol. 4 (12), 127121. <https://doi.org/10.1063/1.4904218/240356>.
- Peters, M., Rüdiger, M., Hauser, H., Hermle, M., Bläsi, B., 2012. Diffraction gratings for crystalline silicon solar cells—optimum parameters and loss mechanisms (Nov.). *Prog. Photovolt.: Res. Appl.* vol. 20 (7), 862–873. <https://doi.org/10.1002/PIP.1151>.
- Trompoukis, C., El Daif, O., Depauw, V., Gordon, I., Poortmans, J., 2012. “Photonic assisted light trapping integrated in ultrathin crystalline silicon solar cells by nanoimprint lithography,” (Sep.). *Appl. Phys. Lett.* vol. 101 (10). <https://doi.org/10.1063/1.4749810/127186>.
- Zhu, L.Q., et al., 2011. Improving the efficiency of crystalline silicon solar cells by an intersected selective laser doping (Dec.). *Sol. Energy Mater. Sol. Cells* vol. 95 (12), 3347–3351. <https://doi.org/10.1016/J.SOLMAT.2011.07.028>.
- Roesch, R., Faber, T., Von Hauff, E., Brown, T.M., Lira-Cantu, M., Hoppe, H., 2015. procedures and practices for evaluating thin-film solar cell stability (Oct.). *Adv. Energy Mater.* vol. 5 (20), 1501407. <https://doi.org/10.1002/AENM.201501407>.
- Lin, L., Ravindra, N.M., 2020. “Temperature dependence of CIGS and perovskite solar cell performance: an overview,” (Aug.). *SN Appl. Sci.* vol. 2 (8), 1–12. <https://doi.org/10.1007/S42452-020-3169-2/FIGURES/6>.
- Nardone, M., Albin, D.S., 2015. Degradation of CdTe solar cells: simulation and experiment (May). *IEEE J. Photo. vol.* 5 (3), 962–967. <https://doi.org/10.1109/JPHOTOV.2015.2405763>.
- Yang, C., Song, K., Xu, X.L., Yao, G., Wu, Z.Y., 2020. Strain dependent effect on power degradation of CIGS thin film solar cell (Jan.). *Sol. Energy* vol. 195, 121–128. <https://doi.org/10.1016/J.SOENER.2019.11.012>.
- Abermann, S., 2013. Non-vacuum processed next generation thin film photovoltaics: Towards marketable efficiency and production of CZTS based solar cells (Aug.). *Sol. Energy* vol. 94, 37–70. <https://doi.org/10.1016/J.SOENER.2013.04.017>.
- Romeo, A., Artegiani, E., 2021. CdTe-based thin film solar cells: past, present and future (Mar.). *Energies* vol. 14 (6), 1684. <https://doi.org/10.3390/EN14061684>.
- Sites, J., Pan, J., 2007. Strategies to increase CdTe solar-cell voltage (May). *Thin Solid Films* vol. 515 (15), 6099–6102. <https://doi.org/10.1016/J.TSF.2006.12.147>.
- Theelen, M., Daume, F., 2016. Stability of Cu(In,Ga)Se<sub>2</sub> solar cells: a literature review (Aug.). *Sol. Energy* vol. 133, 586–627. <https://doi.org/10.1016/J.SOENER.2016.04.010>.
- Liu, F., et al., 2020. Emerging inorganic compound thin film photovoltaic materials: Progress, challenges and strategies (Dec.). *Mater. Today* vol. 41, 120–142. <https://doi.org/10.1016/J.MATTOD.2020.09.002>.
- Galagan, Y., 2020. Perovskite solar cells from lab to fab: the main challenges to access the market (Nov.). *Oxf. Open Mater. Sci.* vol. 1 (1). <https://doi.org/10.1093/OXFMAT/ITAA007>.
- Sun, X., et al., 2023. Synergistic modification of benzimidazole and bromohexyl for highly efficient and stable perovskite solar cells (Feb.). *Chem. Eng. J.* vol. 453, 139698. <https://doi.org/10.1016/J.CEJ.2022.139698>.
- Sieglar, T.D., et al., 2022. The path to perovskite commercialization: a perspective from the United States solar energy technologies office (May). *ACS Energy Lett.* vol. 7 (5), 1728–1734. <https://doi.org/10.1021/ACSENERGYLETT.2C00698>.
- Weerasinghe, H.C., Dkhissi, Y., Scully, A.D., Caruso, R.A., Cheng, Y.B., 2015. Encapsulation for improving the lifetime of flexible perovskite solar cells (Nov.). *Nano Energy* vol. 18, 118–125. <https://doi.org/10.1016/J.NANOEN.2015.10.006>.
- Zhao, Y., Zhou, W., Han, Z., Yu, D., Zhao, Q., 2021a. Effects of ion migration and improvement strategies for the operational stability of perovskite solar cells (Jan.). *Phys. Chem. Chem. Phys.* vol. 23 (1), 94–106. <https://doi.org/10.1039/D0CP04148K>.
- Wang, D., Wright, M., Elumalai, N.K., Uddin, A., 2016. Stability of perovskite solar cells (Apr.). *Sol. Energy Mater. Sol. Cells* vol. 147, 255–275. <https://doi.org/10.1016/J.SOLMAT.2015.12.025>.
- Ma, S., Yuan, G., Zhang, Y., Yang, N., Li, Y., Chen, Q., 2022. Development of encapsulation strategies towards the commercialization of perovskite solar cells (Jan.). *Energy Environ. Sci.* vol. 15 (1), 13–55. <https://doi.org/10.1039/D1EE02882K>.
- Tan, S., et al., 2020. Steric impediment of ion migration contributes to improved operational stability of perovskite solar cells (Mar.). *Adv. Mater.* vol. 32 (11), 1906995. <https://doi.org/10.1002/ADMA.201906995>.
- Sherafatipour, G., et al., 2019. Degradation pathways in standard and inverted DBP-C70 based organic solar cells. *Sci. Rep.* <https://doi.org/10.1038/s41598-019-40541-6>.
- Solak, E.K., Irmak, E., 2023. Advances in organic photovoltaic cells: a comprehensive review of materials, technologies, and performance (Apr.). *RSC Adv.* vol. 13 (18), 12244–12269. <https://doi.org/10.1039/D3RA01454A>.
- Chen, L.X., 2019. “Organic Solar Cells: Recent Progress and Challenges,” (Oct.). *ACS Energy Lett.* vol. 4 (10), 2537–2539. [https://doi.org/10.1021/ACSENERGYLETT.9B02071/ASSET/IMAGES/LARGE/NZ9B02071\\_0002.JPG](https://doi.org/10.1021/ACSENERGYLETT.9B02071/ASSET/IMAGES/LARGE/NZ9B02071_0002.JPG).
- Rahman, M.M., Hasanuzzaman, M., Rahim, N.A., 2017. Effects of operational conditions on the energy efficiency of photovoltaic modules operating in Malaysia (Feb.). *J. Clean. Prod.* vol. 143, 912–924. <https://doi.org/10.1016/J.JCLEPRO.2016.12.029>.
- KatkarA, A., Shinde, N., Patil, P., Tech, M., 2011. “Performance & evaluation of industrial solar cell w.r.t. Temp. Humidity.
- Jiang, H., Lu, L., Sun, K., 2011. Experimental investigation of the impact of airborne dust deposition on the performance of solar photovoltaic (PV) modules (Aug.). *Atmos. Environ.* vol. 45 (25), 4299–4304. <https://doi.org/10.1016/J.ATMOENV.2011.04.084>.
- Abdolzadeh, M., Ameri, M., 2009. Improving the effectiveness of a photovoltaic water pumping system by spraying water over the front of photovoltaic cells (Jan.). *Renew. Energy* vol. 34 (1), 91–96. <https://doi.org/10.1016/J.RENENE.2008.03.024>.
- Elbreki, A.M., Muftah, A.F., Sopian, K., Jarimi, H., Fazlizan, A., Ibrahim, A., 2021. Experimental and economic analysis of passive cooling PV module using fins and planar reflector (Feb.). *Case Stud. Therm. Eng.* vol. 23, 100801. <https://doi.org/10.1016/J.CSITE.2020.100801>.
- Al Tarabshah, A., et al., 2016. Performance of photovoltaic cells in photovoltaic thermal (PVT) modules (Aug.). *IET Renew. Power Gener.* vol. 10 (7), 1017–1023. <https://doi.org/10.1049/IET-RPG.2016.0001>.
- Choubineh, N., Jannesari, H., Kasaeian, A., 2019. Experimental study of the effect of using phase change materials on the performance of an air-cooled photovoltaic system (Mar.). *Renew. Sustain. Energy Rev.* vol. 101, 103–111. <https://doi.org/10.1016/J.RSER.2018.11.001>.
- Hachem, F., Abdulhay, B., Ramadan, M., El Hage, H., El Rab, M.G., Khaled, M., 2017. Improving the performance of photovoltaic cells using pure and combined phase change materials – Experiments and transient energy balance (Jul.). *Renew. Energy* vol. 107, 567–575. <https://doi.org/10.1016/J.RENENE.2017.02.032>.
- Benghanem, M., Al-Mashraqi, A.A., Daffallah, K.O., 2016. Performance of solar cells using thermoelectric module in hot sites (Apr.). *Renew. Energy* vol. 89, 51–59. <https://doi.org/10.1016/J.RENENE.2015.12.011>.
- Hasan, K., Yousuf, S.B., Tushar, M.S.H.K., Das, B.K., Das, P., Islam, M.S., 2022. Effects of different environmental and operational factors on the PV performance: a comprehensive review (Feb.). *Energy Sci. Eng.* vol. 10 (2), 656–675. <https://doi.org/10.1002/ESE3.1043>.
- Elnozahy, A., Rahman, A.K.A., Ali, A.H.H., Abdel-Salam, M., Ookawara, S., 2015. Performance of a PV module integrated with standalone building in hot arid areas as enhanced by surface cooling and cleaning (Feb.). *Energy Build.* vol. 88, 100–109. <https://doi.org/10.1016/J.ENBUILD.2014.12.012>.
- Al Shehri, A., Parrott, B., Carrasco, P., Al Sairi, H., Taie, I., 2017. Accelerated testbed for studying the wear, optical and electrical characteristics of dry cleaned PV solar panels (Apr.). *Sol. Energy* vol. 146, 8–19. <https://doi.org/10.1016/J.SOLAR.2017.02.014>.

- Mani, M., Pillai, R., 2010. Impact of dust on solar photovoltaic (PV) performance: Research status, challenges and recommendations (Dec.). *Renew. Sustain. Energy Rev.* vol. 14 (9), 3124–3131. <https://doi.org/10.1016/J.RSER.2010.07.065>.
- Zhao, W., Lv, Y., Wei, Z., Yan, W., Zhou, Q., 2021b. “Review on dust deposition and cleaning methods for solar PV modules,” (May). *J. Renew. Sustain. Energy* vol. 13 (3). <https://doi.org/10.1063/5.0053866/285068>.
- Assi, A., Hassan, A., Al-Shamisi, M., Hejase, H., 2012. Removal of air blown dust from photovoltaic arrays using forced air flow of return air from air conditioning systems. 2012 Int. Conf. Renew. Energ. Dev. Ctries., REDEC 2012. <https://doi.org/10.1109/REDEC.2012.6416699>.
- Zhi, J., Zhang, L.Z., 2018. Durable superhydrophobic surface with highly antireflective and self-cleaning properties for the glass covers of solar cells (Oct.). *Appl. Surf. Sci.* vol. 454, 239–248. <https://doi.org/10.1016/J.APSUSC.2018.05.139>.
- Liu, W., Ma, H., Walsh, A., 2019. Advance in photonic crystal solar cells (Dec.). *Renew. Sustain. Energy Rev.* vol. 116, 109436. <https://doi.org/10.1016/J.RSER.2019.109436>.
- Bermel, P., et al., 2007. Improving thin-film crystalline silicon solar cell efficiencies with photonic crystals (Dec.). *Opt. Express* vol. 15 (25), 16986–17000. <https://doi.org/10.1364/OE.15.016986>.
- Snaith, H.J., 2013. “Perovskites: The emergence of a new era for low-cost, high-efficiency solar cells,” (Nov.). *J. Phys. Chem. Lett.* vol. 4 (21), 3623–3630. [https://doi.org/10.1021/JZ4020162/ASSET/IMAGES/MEDIUM/JZ-2013-020162\\_0005.GIF](https://doi.org/10.1021/JZ4020162/ASSET/IMAGES/MEDIUM/JZ-2013-020162_0005.GIF).
- Werner, J., et al., 2016b. Efficient monolithic perovskite/silicon tandem solar cell with cell area >1 cm<sup>2</sup> (Jan.). *J. Phys. Chem. Lett.* vol. 7 (1), 161–166. [https://doi.org/10.1021/ACS.JPCLETT.5B02686/SUPPL\\_FILE/JZ5B02686\\_SI\\_001.PDF](https://doi.org/10.1021/ACS.JPCLETT.5B02686/SUPPL_FILE/JZ5B02686_SI_001.PDF).
- Lal, N.N., Dkhissi, Y., Li, W., Hou, Q., Cheng, Y.B., Bach, U., 2017. Perovskite Tandem Solar Cells (Sep.). *Adv. Energy Mater.* vol. 7 (18), 1602761. <https://doi.org/10.1002/AENM.201602761>.
- Al-Ashouri, A., et al., 2020. Monolithic perovskite/silicon tandem solar cell with >29% efficiency by enhanced hole extraction (Dec.). *Science* (1979) vol. 370 (6522), 1300–1309. [https://doi.org/10.1126/SCIENCE.ABD4016/SUPPL\\_FILE/ABD4016\\_AL-ASHOURI\\_SM.PDF](https://doi.org/10.1126/SCIENCE.ABD4016/SUPPL_FILE/ABD4016_AL-ASHOURI_SM.PDF).
- Raza, E., Ahmad, Z., 2022. Review on two-terminal and four-terminal crystalline-silicon/perovskite tandem solar cells: progress, challenges, and future perspectives (Nov.). *Energy Rep.* vol. 8, 5820–5851. <https://doi.org/10.1016/J.EGYR.2022.04.028>.
- Noh, J., Gu, G.H., Kim, S., Jung, Y., 2020. Machine-enabled inverse design of inorganic solid materials: promises and challenges (May). *Chem. Sci.* vol. 11 (19), 4871–4881. <https://doi.org/10.1039/D0SC00594K>.
- Yu, L., Kokkenyesi, R.S., Keszler, D.A., Zunger, A., 2013. Inverse design of high absorption thin-film photovoltaic materials (Jan.). *Adv. Energy Mater.* vol. 3 (1), 43–48. <https://doi.org/10.1002/AENM.201200538>.
- Lu, T., Li, H., Li, M., Wang, S., Lu, W., 2022. “Inverse design of hybrid organic-inorganic perovskites with suitable bandgaps via proactive searching progress,” (Jun.). *ACS Omega* vol. 7 (25), 21583–21594. [https://doi.org/10.1021/ACOSOMEGA.2C01380/ASSET/IMAGES/LARGE/AO2C01380\\_0007.jpeg](https://doi.org/10.1021/ACOSOMEGA.2C01380/ASSET/IMAGES/LARGE/AO2C01380_0007.jpeg) (Jun.).